Biochimie 213 (2023) 66–81

Contents lists available at ScienceDirect

Biochimie

journal homepage: www.elsevier.com/locate/biochi

The *Mycobacterium tuberculosis* protein tyrosine phosphatase MptpA features a pH dependent activity overlapping the bacterium sensitivity to acidic conditions

Michael Kovermann [a], Alessandra Stefan [b, c], Chiara Palazzetti [b], Fabian Immler [a], Fabrizio Dal Piaz [d], Luca Bernardi [e], Valentina Cimone [b], Maria Laura Bellone [f], Alejandro Hochkoeppler [b, c, *]

[a] Department of Chemistry, University of Konstanz, Universitätstraße 10, 78464, Konstanz, Germany
[b] Department of Pharmacy and Biotechnology, University of Bologna, Viale Risorgimento 4, 40136, Bologna, Italy
[c] CSGI, University of Florence, Via della Lastruccia 3, 50019, Sesto Fiorentino, Firenze, Italy
[d] Department of Medicine, University of Salerno, Via Giovanni Paolo II 132, 84084, Fisciano, Italy
[e] Department of Industrial Chemistry "Toson Montanaro", University of Bologna, Viale Risorgimento 4, 40136, Bologna, Italy
[f] Department of Pharmacy, University of Salerno, Via Giovanni Paolo II 132, 84084, Fisciano, Italy

ARTICLE INFO

Article history:
Received 9 February 2023
Received in revised form
3 April 2023
Accepted 24 April 2023
Available online 17 May 2023

Handling Editor: Dr Y Nakamura

Keywords:
Mycobacterium tuberculosis
Protein tyrosine phosphatase
pH
Phosphotyrosine
Competitive inhibitor
Enzyme kinetics

ABSTRACT

The *Mycobacterium tuberculosis* low-molecular weight protein tyrosine phosphatase (MptpA) is responsible for the inhibition of phagosome-lysosome fusion and is essential for the bacterium pathogenicity. This inhibition implies that *M. tuberculosis* is not exposed to a strongly acidic environment *in vivo*, enabling successful propagation in host cells. Remarkably, MptpA has been previously structurally and functionally investigated, with special emphasis devoted to the enzyme properties at pH 8.0. Considering that the virulence of *M. tuberculosis* is strictly dependent on the avoidance of acidic conditions *in vivo*, we analysed the pH-dependence of the structural and catalytic properties of MptpA. Here we show that this enzyme undergoes pronounced conformational rearrangements when exposed to acidic pH conditions, inducing a severe decrease of the enzymatic catalytic efficiency at the expense of phosphotyrosine (pTyr). In particular, a mild decrease of pH from 6.5 to 6.0 triggers a significant increase of $K_{0.5}$ of MptpA for phosphotyrosine, the phosphate group of which we determined to feature a pKa_2 equal to 5.7. Surface plasmon resonance experiments confirmed that MptpA binds poorly to pTyr at pH values < 6.5. Notably, the effectiveness of the MptpA competitive inhibitor L335-M34 at pH 6 does largely outperform the inhibition exerted at neutral or alkaline pH values. Overall, our observations indicate a pronounced sensitivity of MptpA to acidic pH conditions, and suggest the search for competitive inhibitors bearing a negatively charged group featuring p*K*a values lower than that of the substrate phosphate group.

1. Introduction

Mycobacterium tuberculosis is an aerobic pathogenic bacterium representing a major concern for human health, with more than 1.5 million individuals fatally affected worldwide each year. Remarkably, the genus *Mycobacterium* contains both pathogenic and saprophytic bacteria, whose growth is optimal over a narrow and a wide pH interval, respectively [1]. In particular, *M. tuberculosis* suffers of an extremely poor growth when cultured in minimal medium at pH < 6.5 [2]. This very poor growth under acidic conditions, e.g. in Sauton defined medium at pH 6.0, is partially compensated by high concentrations of Mg^{2+} [2]. Nevertheless, *M. tuberculosis* is able to grow at pH 5.7 when cultured in the 7H9 Middlebrook rich medium, albeit both the duplication rate and the biomass yield in this medium are negatively affected by a shift from neutral to acidic pH [3,4]. In addition, it is important to note that the inefficient growth of *M. tuberculosis* under acidic conditions does not necessarily imply that the bacterium cannot survive in low pH

* Corresponding author. Department of Pharmacy and Biotechnology, University of Bologna, Viale Risorgimento 4, 40136, Bologna, Italy.
E-mail address: a.hochkoeppler@unibo.it (A. Hochkoeppler).

https://doi.org/10.1016/j.biochi.2023.04.014

environments. It was indeed observed that, depending on the medium, *M. tuberculosis* withstands exposure to pH 4.5 [5]. In particular, it was shown that the viability of *M. tuberculosis* is fully retained in phosphate-citrate buffer poised at pH 4.5 and supplemented with Tyloxapol [5].

Macrophages are cells of the innate immune system, committed to the degradation of foreign particles. This degradation process is primed by phagocytosis of the target particle, with the phagosomes accordingly formed undergoing a series of maturation steps, i.e., their fusion with early and late endosomes, and finally with lysosomes. When hosted in human cells, *M. tuberculosis* is exposed to acidic conditions occurring in the phagocytic vesicles of macrophages. Interestingly, it was shown that phagosomes undergo acidification after the uptake of *M. tuberculosis*, with an initial fast drop of pH from 7.0 to 6.25 followed by a slow re-alkalinisation to 6.5 [6]. However, this pH is much higher when compared with the values detected in phagosomes fused with lysosomes, i.e., pH $\leq$ 5.0 [7]. In addition, the occurrence of *M. tuberculosis* in infected cultured macrophages was observed to comprise both intact and damaged bacterial cells, with the great majority of intact individuals residing in phagosomes devoid of lysosomal features [8]. More recently, it was shown that cells infected with live *M. tuberculosis* contained phagosomes not fused with lysosomes, whereas the infection with heat-killed bacteria induced the production of phagolysosomes [9]. Further, it was demonstrated that the acidity of phagosomes containing live *M. tuberculosis* or *M. avium* is far from being comparable with that detected in lysosomes [10,11], and that *Mycobacterium*-containing phagosomes are devoid of the vesicular ATPase (vATPase) which is responsible for the acidification of phagosomes [11,12].

M. tuberculosis is known to express the two protein tyrosine phosphatases (PTPases) MptpA (M_r = 17.5 kDa) and MptpB (M_r = 30.2 kDa). It has been shown that the low molecular mass enzyme exclusively exerts its catalytic action at the expense of phosphotyrosine (pTyr) and pTyr-containing peptides and proteins, with phosphoserine and phosphothreonine being rejected as substrates [13]. In addition, it was shown that MptpA is secreted by growing *M. tuberculosis* into the cytosol of host cells [13]. Remarkably, PTPases are known to be engaged in the inception of human infectious diseases [14–17], and it is therefore of interest to note that MptpA is essential for the pathogenicity of *M. tuberculosis* [18]. In particular, MptpA dephosphorylates the host VPS33B (vacuolar protein sorting 33B) protein, which is by this means inactivated [18]. This inactivation prevents, in turn, the phagosome-lysosome fusion [19] conferring virulence to *M. tuberculosis* [20].

A detailed inspection of the catalytic mechanism of PTPases demonstrated that the thiolate group of a cysteine features an unusually low p*Ka* [21] and is essential for the nucleophilic attack to the phosphate group bound to tyrosine [22,23]. This nucleophilic attack is assisted by an essential arginine, as demonstrated with the R409A variant of the *Yersinia* sp. tyrosine phosphatase [24], and by a structural analysis providing evidence that the guanidinium group of R409 interacts with two oxygens of the pTyr phosphate group [25]. In addition, it was observed that both the cysteine and the arginine essential for catalysis are conserved in all PTPases, and that they are spaced by a stretch of five residues, the identity of which can diverge. Therefore, the C(XXXXX)R motif was recognized as the signature for prokaryotic and eukaryotic PTPases, and for both high- and low-molecular mass types, respectively. Moreover, the catalytic action of PTPases requires an amino acid acting first as an acid, and subsequently as a base. In the *Yersinia* sp. PTPase, this requirement is accomplished by an aspartic acid (D356), which transfers a proton to the leaving tyrosine, and subsequently the conjugated aspartate activates a water molecule, generating the secondary nucleophile responsible for the attack to the phosphoenzyme [26]. Noteworthy, the essential cysteine, arginine, and aspartate residues of PTPases are located in loops connecting elements of secondary structure. The loop connecting cysteine and arginine is conventionally denoted as the Phosphate loop, or P-loop, and the stretch of amino acids containing the catalytic aspartate is denominated D-loop. The PTPases strictly specific towards pTyr rely their substrate selection on a hydrophobic pocket designed to locate the phosphate of pTyr in line with the nucleophilic cysteine [25,27], and to trigger an unfavourable geometry for the nucleophilic attack when the phosphate is bound to a shorter amino acid, i.e., serine or threonine [28]. Once pTyr is bound by PTPases, a large conformational rearrangement occurs at the expense of the D-loop. It was indeed shown that this loop moves towards the P-loop by several angstroms, converting the enzyme conformation from an open to a closed, catalytically competent, form [25].

Structurally speaking, both the open and closed form of *M. tuberculosis* MptpA were determined, by means of NMR spectroscopy and X-ray diffraction, respectively [29,30]. Remarkably, the open-to-closed conformational transition of *M. tuberculosis* MptpA shortens the distance between tyrosines Y128 and Y129 (belonging to the D loop) and W48 by more than 10 Å, therefore exposing W48 to different surroundings during catalysis. To take advantage of this, we have constructed the MptpA variant W152F, featuring W48 as the unique tryptophan [31]. Using MptpA W152F, we previously reported that at pH 8 the enzyme features substrate activation, obeys sigmoidal kinetics when the catalytic action is exerted at the expense of pTYr, and that the fluorescence emission of W48 is diagnostic of active site closure [31]. It is important to note that we previously also compared the catalytic action of MptpA with the performance of MptpA W152F, and that we did not observe any significant difference between the wild-type enzyme and the site-specific variant [31]. To further investigate the enzyme properties under conditions to which *M. tuberculosis* is exposed in macrophages, we performed structural and functional assays of MptpA W152F (hereafter denoted $MptpA_{sW48}$) as a function of pH. Accordingly, here we report on the catalytic action and on the overall structural features of $MptpA_{sW48}$ as affected by pH values ranging from 5.0 to 8.0, along with the characterization of the pH-dependent enzyme sensitivity to the competitive inhibitor L335-M34 [32].

2. Materials and Methods

2.1. Materials

All reagents were obtained by Merck-Millipore (Burlington, MA, USA).

2.2. Protein overexpression and purification

The UniProt accession ID for the low-molecular-weight protein tyrosine phosphatase from *Mycobacterium tuberculosis* (MptpA) is P9WIA1. The isoelectric point of MptpA was calculated using the ProtParam software (https://web.expasy.org/protparam). The site-specific variant W152F was overexpressed in *E. coli* BL21(DE3) and purified as previously reported [31]. It is important to note that this variant contains a single tryptophan, i.e., W48, and is thus denoted as $MptpA_{sW48}$. Aliquots of the purified enzyme were stored at −20 °C until used. Enzyme concentration was determined using the Bradford assay [33].

2.3. Activity assays

The catalytic action at the expense of phosphotyrosine (pTyr)

was assayed by a real time ^{31}P high-resolution NMR spectroscopic approach and spectrophotometrically by taking advantage of the different absorption of tyrosine and phosphotyrosine at a wavelength of 282 nm [31]. At this wavelength, the $\Delta\varepsilon_{Tyr\text{-}pTyr}$ was previously determined as equal to 0.96 mM^{-1} cm^{-1} [31]. To test activity as a function of pH, a universal buffer consisting of Tris-HCl and Bis-Tris (25 mM each, and supplemented with 2 mM EDTA), was used. The kinetic parameters of MptpA (K_m, V_{max}, $K_{0.5}$, and Hill coefficient) were calculated with the Levenberg-Marquardt algorithm in SigmaPlot 14 (Systat Software, San Jose, CA). All assays were performed at 20 °C, using a Cary Bio 300 spectrophotometer. The parameter $K_{0.5}$ refers to the substrate concentration corresponding to half-maximal reaction velocity under conditions of sigmoidal kinetics.

2.4. Stopped-flow assays

The conformational changes of MptpA$_{sW48}$ triggered by binding of pTyr were observed by recording the changes in fluorescence emission of the unique enzyme tryptophan (W48). To this aim, a KinTek SF2004 stopped-flow equipment was used, exciting the samples at a wavelength of 290 nm and detecting emission by means of a longpass filter. In addition, the generation of tyrosine triggered by mixing enzyme and pTyr was detected by observing the changes in Absorbance at a wavelength of 290 nm. The path length of the stopped-flow observation cell used is equal to 0.5 cm. All the assays were performed at 37 °C. The enzyme syringe contained 30 μM MptpA$_{sW48}$, and the substrate syringe contained 20 mM pTyr. Both enzyme and substrate solutions were buffered at the desired pH values using Tris-HCl/Bis-Tris (50 mM each), 2 mM EDTA.

2.5. NMR spectroscopy

All one-dimensional ^{1}H NMR spectra have been acquired at a temperature of $T = 298$ K using an Avance III NMR spectrometer operating at $B_0 = 14.1$ T and equipped with a cryogenically cooled TCI probe. The concentration of MptpA$_{sW48}$ has been adjusted to 60 μM using Tris-HCl/Bis-Tris (50 mM each), 150 mM NaCl and 1 mM EDTA as buffer. The enzymatic activity of MptpA has been observed by detecting ^{31}P resonance signals in real time by continuous acquisition of one-dimensional NMR spectra using an Avance Neo NMR spectrometer operating at $B_0 = 18.8$ T equipped with a cryogenically cooled QCI probe. The concentration of enzyme and pTyr has been adjusted to 2 μM and 1.5 mM, respectively, using Tris-HCl/Bis-Tris (50 mM each), 150 mM NaCl, and 1 mM EDTA. All one-dimensional ^{1}H spectra have been directly referenced to the resonance signal originating from trimethylsilylpropanoic acid (TMSP). All one-dimensional ^{31}P spectra have been indirectly referenced using the ratio of gyromagnetic ratios between ^{1}H and ^{31}P while considering the resonance signal originating from TMSP in corresponding ^{1}H spectra. Data analysis of one-dimensional ^{31}P NMR spectra acquired in real time have been performed using mono- as well as bi-exponential functions on resonance signals representing phosphate and pTyr, respectively. Experimental data have been normalized using the maximum of initial (in the case of pTyr) or final (in the case of phosphate) value provided by the function used for data analysis.

2.6. Circular dichroism

CD spectra were recorded over the 200–250 nm wavelength interval at a scan rate equal to 50 nm/min, using a Jasco J-810 spectropolarimeter. Protein samples were in PBS buffer poised at pH values ranging from 6.0 to 8.0, and the bandwidth was set to 1 nm. Sixteen scans per sample were acquired and averaged. In addition, the molar ellipticity of MptpA$_{sW48}$ over a pH interval ranging from 5.0 to 8.0 was evaluated at 222 nm. To this aim, a universal buffer consisting of MES and Tris-HCl (10 mM each) was used.

2.7. Surface plasmon resonance analyses

The effect of changing pH value on the binding of pTyr to MptpA$_{sW48}$ was assayed using a Biacore 3000 instrument (GE-Healthcare, Marlborough, MA, USA) according to procedures previously reported [34]. MptpA$_{sW48}$ was immobilized on research grade CM5 sensor chips (GE-Healthcare) by immobilizing the protein (100 μg/mL in 10 mM CH_3COONa, pH 5.0) using a standard amine coupling protocol, yielding an observed density of 10 kRU. The substrate pTyr was solubilized in HPS-EP buffer (10 mM Hepes pH 7.4, 150 mM NaCl, 3 mM EDTA, and 0.005% (v/v) surfactant P20) and then diluted in HPS-EP buffer poised at different pH values (5.5, 6.0, 6.5, 7.0) to obtain a series of samples at three different concentrations (150, 450, and 1350 nM). Binding experiments were performed at 25 °C, using a flow rate of 10 μL/min, with 400 and 60 s of association and dissociation time, respectively. A single site (1:1 binding) interaction model was fitted to the observed kinetics. The elaboration of sensorgrams was achieved using the BIAevaluation software, provided by GE-Healthcare.

2.8. Synthesis of the L335-M34 competitive inhibitor

The MptpA inhibitor denominated L335-M34 was synthesized according to previously published procedures [32]. Essentially, the appropriate reagents mixture [32] was incubated and stirred for 3 h at room temperature, under nitrogen atmosphere. Afterwards, the first step of L335-M34 purification consisted of an extraction with dichloromethane and H_2O, using a separation funnel. The organic phase was dehydrated with $MgSO_4$, filtered and dried under vacuum. It was serendipitously found that adding dichloromethane and concentrated aqueous HCl to this residue, a white precipitate formed, which was conveniently recovered by filtration. Subsequently, one-dimensional ^{1}H NMR (using a 300 MHz NMR spectrometer, sample dissolved in DMSO-*d*6) and ESI-MS analyses revealed that this white solid consisted in a very pure salt of L335-M34 with 3,5-Dibromo-4-methylanilinium (Supplementary Fig.s S1 and S2). This salt was solubilized in methanol and loaded onto a column containing the acidic resin Dowex 50WX8-11, previously conditioned with methanol. The eluted solution was dried under vacuum, dissolved in CD_3OD and subjected to one-dimensional ^{1}H NMR spectroscopic analysis (300 MHz) analysis, the output of which identified the compound eluted from the column as the desired sulfonic acid product (Supplementary Fig. S3).

2.9. Effect of L335-M34 inhibitor on MptpA$_{sW48}$ activity

Preliminary assays to test the inhibition of MptpA$_{sW48}$ by L335-M34 were performed according to Dutta et al. [32], in the presence of 1 mM *p*-nitrophenyl phosphate (pNPP), 5 nM of enzyme and different concentrations of inhibitor in a universal buffer containing 25 mM Tris-HCl, 25 mM Bis-Tris, and 2 mM EDTA (TBE buffer) at pH 7.0. The hydrolysis of pNPP was spectrophotometrically determined at a wavelength of 405 nm. A control reaction lacking the enzyme was also analysed.

To further test the inhibitory effect of L335-M34, the activity of MptpA$_{sW48}$ was also assayed as a function of inhibitor concentration, in the presence of a constant pTyr concentration (10 mM) in TBE universal buffer at pH 6.0, 7.0, and 8.0, respectively. The enzyme (420 nM) and the inhibitor were incubated for 10 min at

20 °C, then the reactions were started by the addition of pTyr. The enzyme activity at the expense of pTyr was spectrophotometrically assayed at a wavelength of 282 nm. The inhibition exerted by L335-M34 on the MptpA catalytic action was quantitatively inspected according to the equation [35]:

$$\frac{1}{v} = \frac{[S] + K_m}{V_{max}[S]} + \frac{K_m}{V_{max}[S]K_i}[I] \quad (1)$$

where K_i is the inhibition constant, and [I] indicates the concentration of the inhibitor.

2.10. Titration of phosphotyrosine

For the determination of the pKa_2 of the phosphate group of phosphotyrosine, the procedure reported by Bradshaw and Waksman was used [36]. A solution containing 1 mM pTyr in 25 mM Tris-HCl, 25 mM BisTris, 25 mM sodium acetate (pH 8.0) was prepared. Small volumes of 1.33 M acetic acid were added to the pTyr solution in order to decrease, stepwise, the pH of the solution from 8 to approximately 4. After each addition of acetic acid, the pH and the Absorbance (at wavelengths of 269 and 279 nm) were determined. To calculate the pKa_2 of pTyr, the following equation was fit to the experimental observations [36]:

$$\mathrm{Abs} = \frac{(A1 - A2)}{1 + 10^{pKa2 - pH}} + A2 \quad (2)$$

where *A1* and *A2* represent the Absorbance of the deprotonated and the protonated form, respectively.

2.11. Determining the surface electrostatic potential of MptpA

The surface electrostatic potential of MptpA was determined using the APBS plugin of PyMol (release 2.5.2) and the tertiary structure of the enzyme reported by Madhurantakam et al. (PDB file 1u2p, [30]). Calculations were performed taking into account the protein formal charge. Further, an additional state of MptpA was generated by adding a formal positive charge to each of the ten histidines of the enzyme. This MptpA state was also subjected to the estimation of its surface electrostatic potential.

3. Results

3.1. Kinetics of pTyr hydrolysis by $MptpA_{sW48}$ under steady-state conditions

As a first test of the pH-dependence of $MptpA_{sW48}$ catalytic performance, we assayed the enzyme activity at the expense of 10 mM pTyr in the presence of a universal buffer poised at pH values ranging from 5.0 to 8.0. By this means, we observed that $MptpA_{sW48}$ performed best at neutral or slightly acidic pH, with the enzyme activity featuring a bell-shaped dependence on pH (Fig. 1A). In particular, we detected a very poor activity at pH < 6.0, equal to less than 100 nM/s (Fig. 1A). To assess if the effect of pH on MptpA activity mirrored differences in the $\Delta\varepsilon_{\mathrm{Tyr\text{-}pTyr}}$ at 282 nm (see Methods) we determined the absorbance spectra of tyrosine and pTyr at pH 6.0, 7.0, and 8.0. Over this pH interval, no significant differences were detected neither among the spectra of tyrosine nor among those of pTyr (Supplementary Fig. S4), indicating that the bell-shaped curve of MptpA activity as a function of pH is diagnostic of the enzyme performance. To analyze in detail how the catalytic action of $MptpA_{sW48}$ is affected by pH, we then determined the enzyme kinetic parameters over the 6–8 pH interval, using pTyr as substrate. Remarkably, $MptpA_{sW48}$ obeyed sigmoidal kinetics at pH values from 6.5 to 8.0, featuring Hill coefficients ranging from 1.6 ± 0.2 to 2.2 ± 0.2 (Fig. 1C–F, Table 1). Further, over this pH interval we detected an essentially constant $K_{0.5}$ for pTyr, whereas we determined significant differences among V_{max} values, with a maximum observed at pH 7 (Fig. 1C-1F, Table 1). Surprisingly, activity assays performed at pH 6.0 revealed that $MptpA_{sW48}$ obeyed Michaelis-Menten kinetics, with values for $K_{0.5}$ and V_{max} much higher than those obtained at pH 6.5–8.0 (Fig. 1B, Table 1). In particular, V_{max} was observed to undergo a rather limited enhancement, whereas $K_{0.5}$ was observed to feature a significant increase, i.e. from 2-3 to 55 mM (Table 1). To further test the magnitude of this large increase of $K_{0.5}$ at pH 6.0, we performed an additional independent experiment, the outcome of which yielded $K_{0.5}$ and V_{max} values equal to 90 ± 50 mM and 2038 ± 1007 nM/s, respectively (Supplementary Fig. S5). Accordingly, upon the decrease of pH from 6.5 to 6.0 the enzyme not only faces a sharp transition from sigmoidal to Michaelis-Menten kinetics, but does also suffer of a very high K_m value, which limits the catalytic efficiency of $MptpA_{sW48}$. At first glance, a similar change in enzyme performance could be ascribed to considerable denaturation. However, it should be noted that at pH 6.0, in the presence of 15 mM pTyr, $MptpA_{sW48}$ features an activity level comparable to those detected at pH values ranging from 6.5 to 7.5 (Fig. 1B–F). To investigate this point in greater detail, we performed three additional activity assays at pH 6.0 in the presence of 420 nM enzyme and 15 mM pTyr, obtaining a mean value equal to 271 ± 22 nM/s (cf. Fig. 1B–F). Therefore, the conformational transitions to which the enzyme is subjected at pH 6.0 do not compromise its catalytic action. Nevertheless, activity assays performed at pH values lower than 6 revealed that the hydrolysis of pTyr by $MptpA_{sW48}$ occurred rather slowly, therefore hampering a quantitative evaluation of the enzyme kinetic parameters under this condition (Fig. 1A).

3.2. The pKa_2 of the phosphate group of phosphotyrosine

The observation that the $K_{0.5}$ value of $MptpA_{sW48}$ for phosphotyrosine pronouncedly increases when the pH is lowered from 6.5 to 6.0 prompted us to investigate the ionization state of this phosphorylated amino acid as a function of pH. In particular, we performed a spectroscopic assay over a pH interval which is diagnostic of the pKa_2 of pTyr phosphate group, as previously reported by Bradshaw and Waksman for a pTyr-containing peptide [36]. First, and to discriminate between the ionized and the neutral form of pTyr phosphate group, we recorded the absorbance spectra of phosphotyrosine solubilized in 1 M HCl or in 1 M NaOH. By this means, we observed that pTyr dissolved under alkaline conditions features a higher molar absorptivity over the 265–285 nm wavelength interval when compared to the same concentration of pTyr solubilized in the acidic solution (Fig. 2A). This is in agreement with previous observations obtained with pTyr-containing solutions whose pH values were equal to 1 or 13 [37]. In particular, we detected three maxima in the difference spectrum, respectively located at a wavelength of 269, 274, and 279 nm (Fig. 2B). Accordingly, by using acetic acid we stepwise titrated a solution of 1 mM pTyr dissolved in a universal buffer poised at pH 8.0, and we concomitantly determined the changes in Absorbance at a wavelength of 269 and 279 nm. By this means, and fitting the equation reported by Bradshaw and Waksman [36] (see Methods) to our experimental observations, we determined pKa_2 values for the pTyr phosphate group equal to 5.76 ± 0.01 and 5.67 ± 0.01, for λ = 269 and 279 nm, respectively (Fig. 2C). Interestingly enough, this implies that the large increase of $K_{0.5}$ observed when the pH is lowered from 6.5 to 6.0 (Table 1) is related to a 3-fold decrease of the charged/uncharged molar ratio of the pTyr phosphate group. This suggests that the presence of a negative charge in the pTyr

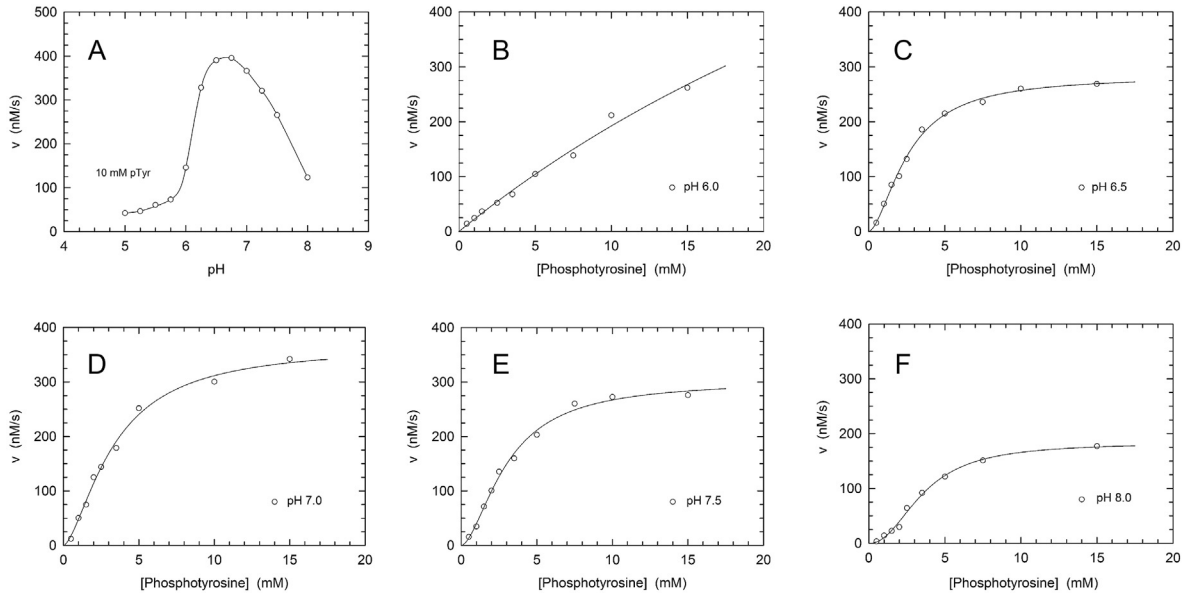

Fig. 1. Steady-state activity of MptpA$_{sW48}$ at the expense of phosphotyrosine under different pH conditions
(**A**) Initial reaction velocity determined as a function of pH using assay mixtures containing 420 nM MptpA$_{sW48}$, 10 mM pTyr, 2 mM EDTA, and a universal buffer consisting of Tris-HCl and Bis-Tris, 25 mM each. The continuous line is used as a guide to the eye. (**B**–**F**) Dependence of the MptpA$_{sW48}$ catalytic action on substrate concentration and pH at the expense of phosphotyrosine, in the presence of 420 nM enzyme. Other conditions as in panel A. Assays were performed at pH 6.0, 6.5, 7.0, 7.5, and 8.0 (panels B to F, respectively). The continuous lines represent the best fit of the Michaelis-Menten or the Hill equation to the experimental observations. See Table 1 for the corresponding numerical data.

Table 1
Kinetic parameters of MptpA$_{sW48}$ determined as a function of pH under steady-state conditions.
The corresponding data are shown in Fig. 1.

pH	V_{max} (nM/s)	$K_{0.5}$ (mM)	Hill
6.0	1250 ± 450	55 ± 25	–
6.5	280 ± 10	2.6 ± 0.1	1.7 ± 0.1
7.0	370 ± 20	3.3 ± 0.3	1.6 ± 0.2
7.5	300 ± 10	3.0 ± 0.2	1.7 ± 0.2
8.0	180 ± 5	3.6 ± 0.2	2.2 ± 0.2

phosphate group does strongly favour substrate binding.

3.3. Dissociation of the pTyr-MptpA$_{sW48}$ complex as a function of pH

To further inspect the effects triggered by a change of pH on the binding of pTyr to MptpA$_{sW48}$, we performed Surface Plasmon Resonance (SPR) assays. In particular, MptpA was immobilized on a sensor chip and we analysed the binding events occurring when the immobilized enzyme was exposed to different concentrations of pTyr at pH values ranging from 5.5 to 7.0. We detected significant differences in the extent of pTyr binding by MptpA$_{sW48}$, with pH 7.0 being the more favourable condition for the association of enzyme and substrate (Fig. 3, Table 2). However, we note that the K_D values evaluated at pH 7.0 and 6.5 represent the outcome of quite different contributions by the association and dissociation rate constants (Table 2). In particular, the k_{off} value is lower at pH 6.5 (k_{off} = 1.5 ± 0.3•10^{-3} s^{-1}, Table 2) compared to the value determined at pH 7.0. This implies that MptpA features a more efficient binding of pTyr at pH 7, and that the enzyme-substrate complex is tighter at pH 6.5 Remarkably, at pH ≤ 6.5 the K_D value of the MptpA-pTyr complex undergoes a sharp increase when compared to the values determined under neutral conditions (Fig. 3, Table 2). In particular, the extent of this increase at pH 5.5–6.0 is too high to quantitatively evaluate the binding of pTyr to MptpA$_{sW48}$ (Fig. 3 A-B, Table 2). Overall, the observations obtained by the SPR assays suggest that the stability of the pTyr-MptpA complex is greatly affected by the ionization state of the pTyr phosphate group, with dissociation greatly favoured at pH values lower than the pKa_2 of the substrate phosphate group.

3.4. Stopped-flow assays of enzyme conformational transitions triggered by pTyr binding under different pH conditions

To analyze the pH-dependence of MptpA$_{sW48}$ catalytic action under pre-steady-state conditions, we took advantage of the presence of the single tryptophan in MptpA$_{sW48}$. In particular, tandem stopped-flow assays were performed to detect: i) the generation of tyrosine, by observing the changes of Absorbance at 290 nm triggered by mixing enzyme and substrate (tyrosine does indeed feature absorptivity at this wavelength whereas pTyr does not, see Supplementary Fig. S4); ii) the changes of fluorescence emission of the enzyme tryptophan induced by pTyr binding. Surprisingly, when tested at pH 6.0 the reaction at the expense of pTyr occurs at a rather modest, if at all, extent. We indeed observed an initial decrease in Absorbance (lasting for about 10 s after mixing enzyme and substrate), with a subsequent increase of Absorbance the amplitude of which was less than 0.0015 over a 50 s time-interval (Fig. 4A). An appropriate equation containing an exponential and a linear component can be reasonably fitted to these experimental observations, yielding the kinetic rate constants for the initial (Absorbance decrease) and the subsequent (Absorbance increase) phase, respectively (Table 3). Taking a $\Delta\varepsilon_{Tyr\text{-}pTyr}$ at λ = 290 nm equal to 0.14 ± 0.02 mM^{-1}cm^{-1} into account (Supplementary Fig. S4), the detected rate constant for the increase in Absorbance corresponds to 366 nM/s of tyrosine generated in the presence of 15 μM enzyme. When changes of emission of fluorescence triggered by mixing enzyme and pTyr at pH 6.0 are considered, we observed an initial exponential decay of limited amplitude (Fig. 4A, magenta circles, Table 3) which is followed by a linear decrease in fluorescence (Fig. 4A, cyan circles, Table 3). To interpret the observations obtained at pH 6.0, we propose that: i) the initial

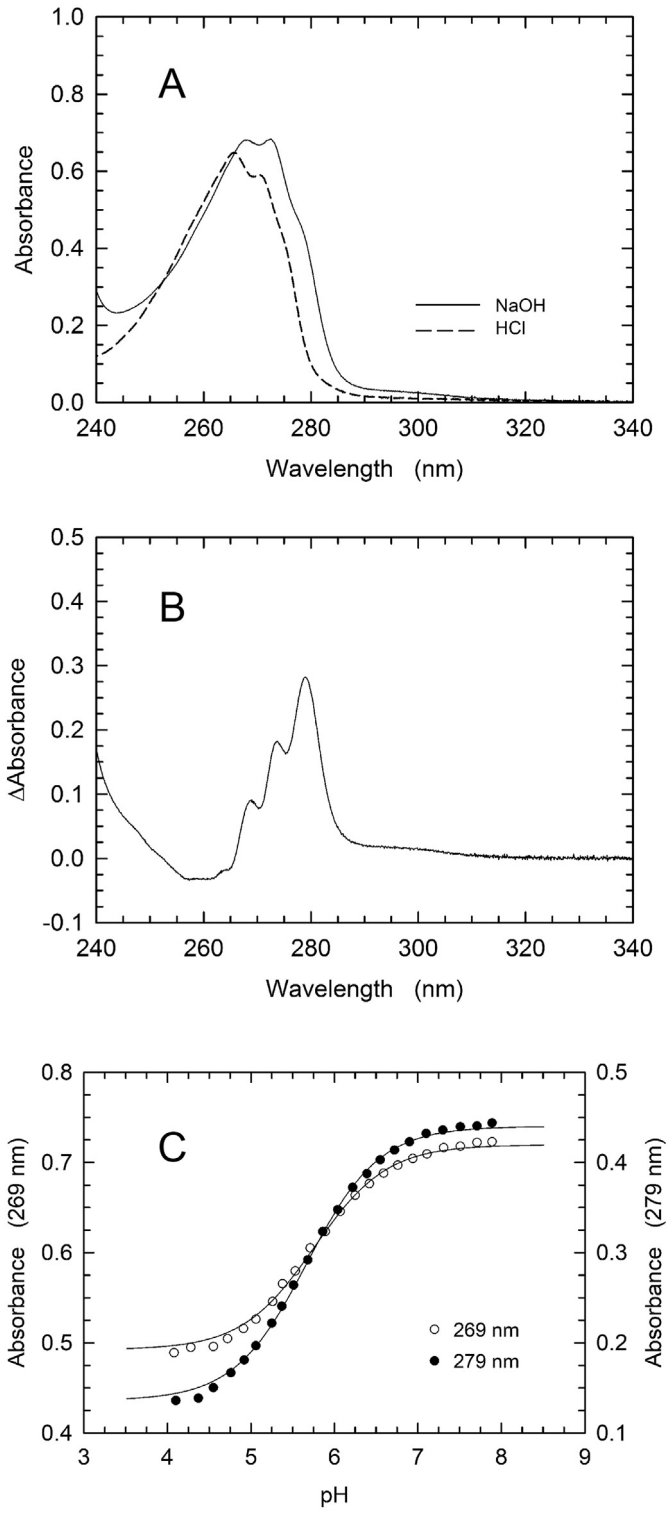

Fig. 2. Determination of the pKa_2 of the phosphate group of phosphotyrosine
(**A**) Absorbance spectra of 1 mM phosphotyrosine solubilized in 1 M NaOH (continuous line) or in 1 M HCl (dashed line). (**B**) Difference between the absorption spectra of 1 mM pTyr obtained under alkaline and acidic conditions. (**C**) Titration of the pTyr phosphate group monitoring the changes in Absorbance induced at a wavelength of 269 and 279 nm (empty and filled circles, respectively) by stepwise additions of acetic acid to a phosphotyrosine-containing solution poised at pH 8.0 (see Methods for details). The continuous lines represent the best fit of the equation reported by Bradshaw and Waksman (see Methods) to the experimental observations.

decrease of Absorbance represents binding of pTyr to $MptpA_{sW48}$, the occurrence of which translates into a reduced absorptivity of the enzyme aromatic amino acids; ii) the exponential decrease of fluorescence emission is diagnostic of enzyme closure, with the single tryptophan probing this conformational transition; iii) the linear increase in Absorbance and decrease of fluorescence emission, both occurring 10 s after mixing enzyme and substrate, do slowly lead to the attainment of a steady-state hydrolysis of pTyr and tryptophan fluorescence, respectively. Remarkably, increasing pH from 6.0 to 7.0 gave rise to a largely improved pre-steady-state catalytic action of $MptpA_{sW48}$. First, the lag phase occurring at pH 6.0 (before the generation of product) was not detected at pH 7.0. Moreover, both the increase of absorbance and the decrease of fluorescence emission triggered by enzyme and substrate mixing can be considered as rather fast processes at pH 7.0, appropriately accounted for by fitting a double-exponential equation to the experimental observations (Fig. 4B, Table 3). Interestingly, when enzyme and substrate were mixed at pH 8 we detected an exponential rise of Absorbance and an exponential decay of fluorescence emission, indicating that shifting the pH to values above or below 7.0 triggers quite different effects on the pre-steady-state catalytic action of $MptpA_{sW48}$ (cf. Fig. 4A and 4C). In addition, it should be noted that differences of significance were determined for the kinetic rate constants obtained at pH 7.0 and 8.0 (Table 3). Moreover, at pH 7.0 the pre-steady-state amplitude of the Absorbance changes linked to product generation was one order of magnitude higher than the corresponding amplitude detected at pH 8.0 (cf. Fig. 4B and 4C). This was confirmed by assaying the generation of tyrosine at pH 8 over a shorter time interval, i.e. 10 s (Supplementary Fig. S6). Indeed, the amplitude of the Absorbance changes detected under this condition indicate that by selecting a time interval equal to 60 s we did not omit early (and fast) events occurring at the onset of the reaction (cf. Fig. 4C with Fig. S6).

3.5. Competitive inhibition of $MptpA_{sW48}$

Tuberculosis is usually treated with multi-drug therapies, appropriately tailored to target latent or active disease [38]. However, the emergence of *M. tuberculosis* strains resistant to current treatments is a major concern, which therefore demands for new anti-tuberculosis drugs. Recently, a potent competitive inhibitor of MptpA, denoted L335-M34, was synthesized and its action was tested both *in vitro* and *in vivo* [32]. In particular, the action of this inhibitor at pH 7.0 was evaluated *in vitro* using *p*-nitrophenyl phosphate (pNPP) as substrate [32]. In addition, it was shown that when L335-M34 and the MptpB inhibitor L01-Z08 were used in combination with isoniazid, rifampicin, and pyrazinamide, the therapeutic effectiveness of this standard ternary treatment was significantly improved [32]. However, the effect of pH on the potency of L335-M34 was not investigated *in vitro*, and we were therefore prompted to assay its action as a function of pH. First, L335-M34 was tested under assay conditions similar to those previously used [32], i.e. 5 nM enzyme, 1 mM pNPP, pH 7.0. By this means, we detected a steep decrease of activity in the presence of L335-M34 concentrations up to 100 nM, with this particular concentration responsible for a decrease of about 50% of $MptpA_{sW48}$ activity (Fig. 5A). Qualitatively speaking, this is in reasonable agreement with the IC_{50} value equal to about 160 nM previously reported [32]. We then decided to test the inhibition exerted by L335-M34 on the $MptpA_{sW48}$ catalytic action at the expense of pTyr, under different pH conditions. Further, we selected 10 mM as the concentration of pTyr to be used in these assays, i.e. a concentration higher than the enzyme $K_{0.5}$ at pH values > 6.0, and 5-fold lower

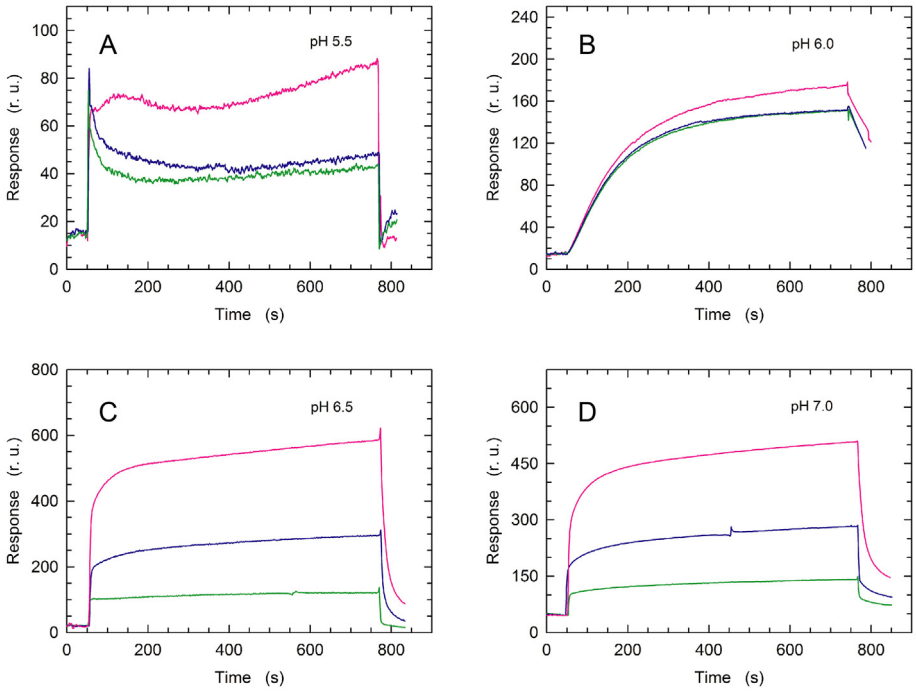

Fig. 3. Surface Plasmon Resonance assays of pTyr binding to MptpA$_{sW48}$
(**A-D**) Sensorgrams observed by loading 150, 450, and 1350 nM phosphotyrosine (green, blue, and magenta lines, respectively) on a sensor chip modified with immobilized MptpA$_{sW48}$. The binding assays were performed at pH 5.5, 6.0, 6.5, and 7.0 (panels A to D, respectively). See Table 2 for the corresponding numerical data.

Table 2
Effect of pH on the thermodynamic and kinetic dissociation constants accounting for the interaction between pTyr and MptpA$_{sW48}$ evaluated by Surface Plasmon Resonance. The corresponding data are shown in Fig. 3.

pH	K_D (M)	k_{off} (s^{-1})
7.0	$(3.9 \pm 0.3)\bullet10^{-7}$	$(4.9 \pm 0.3)\bullet10^{-3}$
6.5	$(6.8 \pm 0.4)\bullet10^{-7}$	$(1.5 \pm 0.3)\bullet10^{-3}$
6.0	Weak binding	–
5.5	Binding not detected	–

than the MptpA$_{sW48}$ $K_{0.5}$ at pH 6.0 (Table 1). A similar inhibition of MptpA$_{sW48}$ activity was observed at pH 7.0 and 8.0, and under both these conditions the enzyme action was approximately halved in the presence of 600 nM inhibitor (Fig. 5B). To quantitatively assess the competitive inhibition exerted by L335-M34, an equation relating the reciprocal of reaction velocities as a function of inhibitor concentration was used (see Methods) [35]. By this means, K_i values equal to 190 ± 15 and 80 ± 10 nM for the inhibition by L335-M34 at pH 7.0 and 8.0, respectively, were determined (Fig. 5C). It should be noted that these numerical values were obtained by fitting a linear equation to the experimental observations in the absence of any constraints. Therefore, not only the slope (accounting for K_i) but also the intercept was determined by the fitting procedure. Consequently, a direct comparison between the expected value of the intercept (calculated with the K_m and V_{max} data reported in Table 1, and using [S] = 10 mM) with the value determined by this fitting procedure represents a reliability test of the enzyme kinetic parameters. Notably, considering the inhibition assay at pH 7.0, numerical values equal to 0.0036 and 0.0034 s/nM for the expected and the fitting-determined intercept were obtained (Table 1 and Fig. 5C). Further, a reasonable agreement was also obtained for the inhibition experiment carried out at pH 8.0, with expected and determined values of 0.0074 and 0.0062 s/nM, respectively (Table 1 and Fig. 5C). Interestingly, when the inhibition assay was performed at pH 6 using 10 mM pTyr, we detected an activity of MptpA$_{sW48}$ equal to 120 and 25 nM/s in the absence and in the presence of 200 nM L335-M34, respectively (Fig. 5D). This strength of inhibition is much larger when compared to the effects observed at pH 7 or 8 (Fig. 5B), indicating that the competitive inhibitor L335-M34 is more effective under pH conditions that can be considered as unfavourable for substrate binding (Tables 1 and 2). In particular, it should be considered that in the presence of 10 mM substrate (Fig. 5D) the high value of K_m for pTyr at pH 6.0 (55 mM, Table 1) translates into a concentration of the ES complex much lower than the total enzyme concentration. This, in turn, implies that L335-M34 can strongly inhibit MptpA$_{sW48}$ at inhibitor/enzyme molar ratios <0.5 (Fig. 5D). Finally, it should be noted that the slow rate of the reaction at pH 6.0 hampers the determination of a reliable K_i value at this pH.

3.6. Structural and functional insights on MptpA$_{sW48}$ obtained by NMR spectroscopy

We have also made profit by using high-resolution NMR spectroscopy to probe the catalytic action of MptpA$_{sW48}$ at the expense of pTyr. Specifically, one-dimensional ^{31}P NMR spectra have been obtained as a function of time, enabling to determine the kinetics of pTyr consumption and the concomitant generation of phosphate for pH values equal to 7.0, 7.5 and 8.0 (Fig. 6). Remarkably, significant displacements of the chemical shifts corresponding to pTyr and phosphate resonance signals were detected as a function of both pH and substrate/product concentration (Fig. 6). Whereas a rather fast exchange process can be seen for pH 7.0 and 7.5, both the consumption of pTyr and the generation of phosphate by MptpA$_{sW48}$ at pH 8.0 is not accompanied by changes in chemical shifts. It is likely that the dependence of the association and dissociation rate constant and thus the affinity between phosphate/pTyr and MptpA$_{sW48}$ on the pH value is responsible for the spectroscopic differences of the ^{31}P signal detected here. Moreover, the

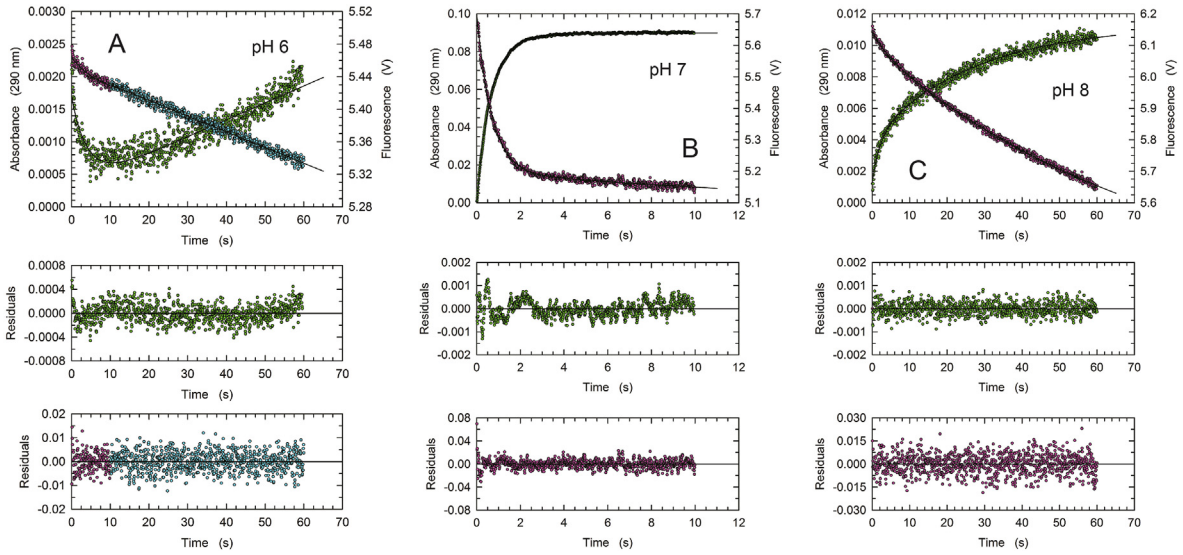

Fig. 4. Stopped-flow assays of the pre-steady-state activity of MptpA$_{sW48}$ at the expense of phosphotyrosine under different pH conditions.
(**A**) Changes in Absorbance (green dots) and fluorescence (magenta and cyan dots) induced by mixing 15 μM MptpA$_{sW48}$ with 10 mM phosphotyrosine, at pH 6.0. The continuous lines represent the best fits of appropriate equations to the experimental observations. (**B**) Changes in Absorbance (green dots) and fluorescence (magenta dots) induced by mixing, at pH 7.0, 15 μM MptpA$_{sW48}$ with 10 mM phosphotyrosine. The continuous lines represent fits of a double-exponential equation to the experimental observations. (**C**) Changes in Absorbance (green dots) and fluorescence (magenta dots) induced by mixing, at pH 8.0, 15 μM MptpA$_{sW48}$ with 10 mM phosphotyrosine. The continuous lines represent fits of a double-exponential equation to the experimental observations. See Table 3 for the corresponding numerical data.

Table 3
Kinetic rate constants (in units of seconds) and amplitudes determined by fitting the indicated equations to the experimental observations obtained by mixing MptpA$_{sW48}$ and pTyr under pre-steady-state conditions at pH 6, 7, and 8.
The corresponding data are shown in Fig. 4.

pH 6.0	pH 7.0	pH 8.0
Absorbance, $f = y_0 + a \bullet \exp^{-bx} + c \bullet x$	**Absorbance, $f = y_0 + a \bullet (1-\exp^{-bx}) + c \bullet (1-\exp^{-dx})$**	**Absorbance, $f = y_0 + a \bullet (1-\exp^{-bx}) + c \bullet (1-\exp^{-dx})$**
$y_0 = (3.0 \pm 0.2) \bullet 10^{-4}$	$y_0 = (-10.0 \pm 1.3) \bullet 10^{-4}$	$y_0 = (10 \pm 1) \bullet 10^{-4}$
$a = (100 \pm 4) \bullet 10^{-5}$	$a = 0.042 \pm 0.003$	$a = (30 \pm 1) \bullet 10^{-4}$
$b = 0.25 \pm 0.01$	$b = 2.26 \pm 0.08$	$b = 0.49 \pm 0.04$
$c = (260 \pm 5) \bullet 10^{-7}$	$c = 0.049 \pm 0.003$	$c = (700 \pm 5) \bullet 10^{-5}$
Fluorescence (0–10 s), $f = y_0 + a \bullet \exp^{-bx}$	$d = 1.11 \pm 0.02$	$d = 0.036 \pm 0.001$
$y_0 = 5.418 \pm 0.005$	**Fluorescence, $f = y_0 + a \bullet \exp^{-bx} + c \bullet \exp^{-dx}$**	**Fluorescence, $f = y_0 + a \bullet \exp^{-bx} + c \bullet \exp^{-dx}$**
$a = 0.046 \pm 0.004$	$y_0 = 5.0 \pm 0.2$	$y_0 = 5.28 \pm 0.02$
$b = 0.14 \pm 0.03$	$a = 0.504 \pm 0.003$	$a = 0.047 \pm 0.002$
Fluorescence (10–60 s), $f = y_0 + a \bullet x$	$b = 1.43 \pm 0.02$	$b = 0.29 \pm 0.03$
$y_0 = 5.5 \pm 3.7 \bullet 10^{-4}$	$c = 0.18 \pm 0.16$	$c = 0.82 \pm 0.01$
$a = -(2000 \pm 10) \bullet 10^{-6}$	$d = 0.03 \pm 0.03$	$d = 0.0130 \pm 0.0004$

observed ^{31}P spectra indicate that the slowest rate constant related to pTyr hydrolysis occurs at pH 8.0 (Fig. 6). Further, the decrease (for pTyr) and the increase (for phosphate) of signal heights observed in the ^{31}P spectra was analysed as a function of time by using a double- or a single-exponential function (Fig. 7). Interestingly, these analyses revealed that: i) when the reaction was assayed at pH 7.0 or 7.5 a fast and a slow phase were detected, with the fast phase dominating the amplitude at pH 7.0 (Fig. 7 A-D, Table 4); ii) at pH 8.0, pTyr hydrolysis can be interpreted as a slow process, conveniently accounted for by a single phase (Fig. 7 E-F, Table 4). We also note that the numerical values of the rate constants determined for the decay of pTyr are in good agreement with those calculated for generation of phosphate (Table 4 and Supplementary Fig. S7).

To get insights into structural features of MptpA$_{sW48}$ at atomic resolution we used NMR spectroscopy, and we considered the potential dependence on pH conditions of enzyme secondary and tertiary structure. First, one-dimensional ^{1}H NMR spectra have been acquired enabling to precisely probe overall structural characteristics (the tertiary fold of MptpA$_{sW48}$) when proton signals are analysed for chemical shifts arising in the high field region (Fig. 8). The decrease of pH from 8.0 to 6.0 shifts MptpA$_{sW48}$ from well-structured conformations to an ensemble of rather disordered conformations known from folding-to-unfolding studies performed on proteins exposed to urea or to temperature values inducing denaturation [39,40]. Specifically, MptpA$_{sW48}$ can be classified as a properly folded enzyme over the pH interval from 7.0 to 8.0, as indicated by the integral determined for resonance signals arising in the range of chemical shifts exclusively observed for properly folded proteins (Fig. 8A and 8C). In addition, the decrease of pH to values $\leq$ 6.5 triggers a considerable drop of this pattern of resonance signals, suggesting a significant loss of MptpA$_{sW48}$ tertiary structure (Fig. 8A and 8C). This series of NMR experiments has been repeated in the presence of pTyr, leading to comparable observations (Fig. 8B and 8C). We have also determined ^{31}P one-dimensional NMR spectra of pTyr in the presence of MptpA$_{sW48}$ over a pH interval ranging between 5.0 and 8.0 (Fig. 8D). Here, prominent changes in the chemical shifts of the pTyr resonance signal occur at pH $\leq$ 6.5 when compared to the corresponding signals detected at 6.75 $\leq$ pH $\leq$ 8.0 (Fig. 8D). In particular, pTyr is

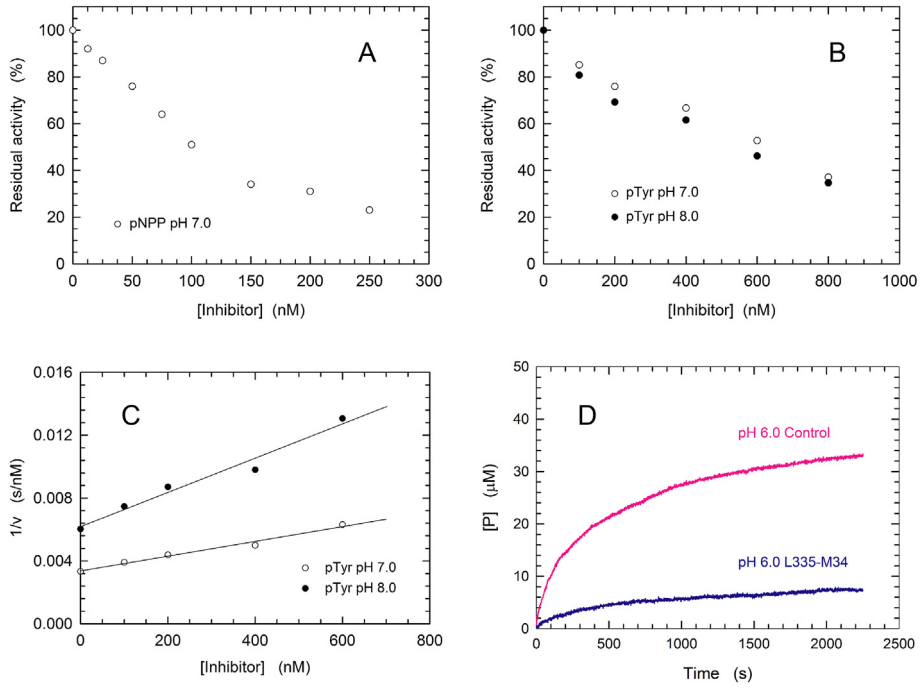

Fig. 5. Competitive inhibition of MptpA$_{sW48}$ catalytic action by L335-M34
(**A**) Inhibition of MptpA$_{sW48}$ activity at the expense of *p*-nitrophenyl phosphate (pNPP) in the presence of 5 nM enzyme, 1 mM substrate, at pH 7.0. (**B**) Catalytic action of MptpA$_{sW48}$ exerted on pTyr in the presence of the competitive inhibitor L335-M34. Two series of assays were performed, at pH 7.0 and 8.0, respectively. The catalytic activity was tested in the presence of 420 nM enzyme, and 10 mM phosphotyrosine. (**C**) Analysis of the data reported in Fig. 5B to estimate the value of the inhibition constant K_i of L335-M34 at pH 7.0 (empty circles) and pH 8.0 (filled circles). A linear equation was used to analyze the experimental observations, with the slopes accordingly determined containing K_i as a free parameter used in the fitting procedure (see Methods). (**D**) Kinetics of phosphotyrosine hydrolysis catalyzed by 420 nM MptpA$_{sW48}$ in the presence of 10 mM substrate, at pH 6.0. Activity assays were performed in the absence or in the presence of 200 nM L335-M34 (magenta and blue line, respectively).

rather mildly affected when the pH is lowered from 6.75 to 6.5, as suggested by the modest change ($\delta \cong 0.25$ ppm) of the chemical shift of the resonance signal of pTyr. On the contrary, lowering the pH from 6.5 to 6.0, from 6.0 to 5.5 or even from 5.5 to 5.0 induces larger changes ($\delta = 0.65$, 0.9, and 0.65 ppm, respectively) in the chemical shift of the resonance signal of pTyr, suggesting rather prominent conformational rearrangements of pTyr (Fig. 8D). In summary, pTyr features a rather broad pattern in chemical shifts ($\delta = 2.2$ ppm) when the pH is lowered from 6.5 to 5.0 in contrast to the moderate $\delta = 0.4$ ppm determined over the pH interval ranging from 8.0 to 6.5.

It should be noted that we acquired one-dimensional ^{1}H NMR spectra over pH values ranging from 5.0 to 8.0, and that the theoretical isoelectric point of MptpA is equal to 6.03 (see Methods). Accordingly, the signal height of resonance signals arising in these NMR spectra (Fig. 8A and 8B) could be potentially affected by the solubility of MptpA$_{sW48}$. Therefore, two series of MptpA$_{sW48}$ solutions, prepared to contain 5 or 50 μM enzyme and poised at pH 5.0, 5.5, 6.0, 6.5, 7.0, 7.5 were incubated for 24 h at room temperature. At the end of the incubation, all samples were centrifuged (13,000×*g*, 20 min), the protein concentration of the supernatants accordingly obtained was determined and then compared with the assayed starting concentration. By this means, we observed the following (Supplementary Fig. S8): i) samples containing 5 μM MptpA$_{sW48}$ and featuring pH values ranging from 6.0 to 7.5 proved to be very stable, as indicated by a very limited, if at all, decrease of protein concentration after 24 h of incubation; ii) samples prepared at pH 5.0 and 5.5 and containing 5 μM MptpA$_{sW48}$ did face a decrease (equal to 40 and 30%, respectively) of protein concentration; iii) remarkably, when the samples containing 50 μM MptpA$_{sW48}$ are considered, we observed a decrease of protein concentration in the enzyme solution prepared at pH 6.5; iv) furthermore, the samples poised at pH 6.0 (i.e. at a pH value very close to the theoretical pI of MptpA) and at pH 7.0 underwent a similar decrease in protein concentration. Overall, these observations suggest that the different patterns detected for MptpA$_{sW48}$ in 1D^{1}H NMR spectra (Fig. 8A and 8B) are not induced by effects of pH on enzyme solubility. Further, this is supported by analyzing the integrals determined for the resonance signals arising between 5.86 and 10.55 ppm in the 1D^{1}H NMR spectra of MptpA$_{sW48}$ observed as a function of pH (Supplementary Fig. S9). Indeed, whereas the overall pattern of the signals originated by amide and aromatic protons changes when the pH shifts below 6.75, the numerical value of the integral of the signals does not feature a significant pH-dependence (Supplementary Fig. S9). Accordingly, it can be concluded that the amount of soluble MptpA$_{sW48}$ molecules is not affected when the pH is lowered down to 5.0. Qualitatively speaking, MptpA$_{sW48}$ is subjected to important conformational rearrangements when the pH is shifted below 6.75. Actually, the well-resolved resonance signals detected in the 1D^{1}H NMR spectra acquired over pH values ranging from 8.0 to 6.75 disappear at lower pH values and contribute to a rather broad overall shape of the 1D^{1}H NMR spectrum (Supplementary Fig. S9). We interpret these observations as related to a structural transition of MptpA$_{sW48}$ from a properly folded to a molten globule state.

3.7. Analysis of MptpA$_{sW48}$ structural properties by CD spectroscopy

To determine to what extent the secondary structure of MptpA$_{sW48}$ is affected by pH, far UV CD spectra of the enzyme over a pH interval ranging from 6.0 to 8.0 were acquired. Interestingly, we observed relatively invariant spectra at pH values ≥ 7.0 (Fig. 9A).

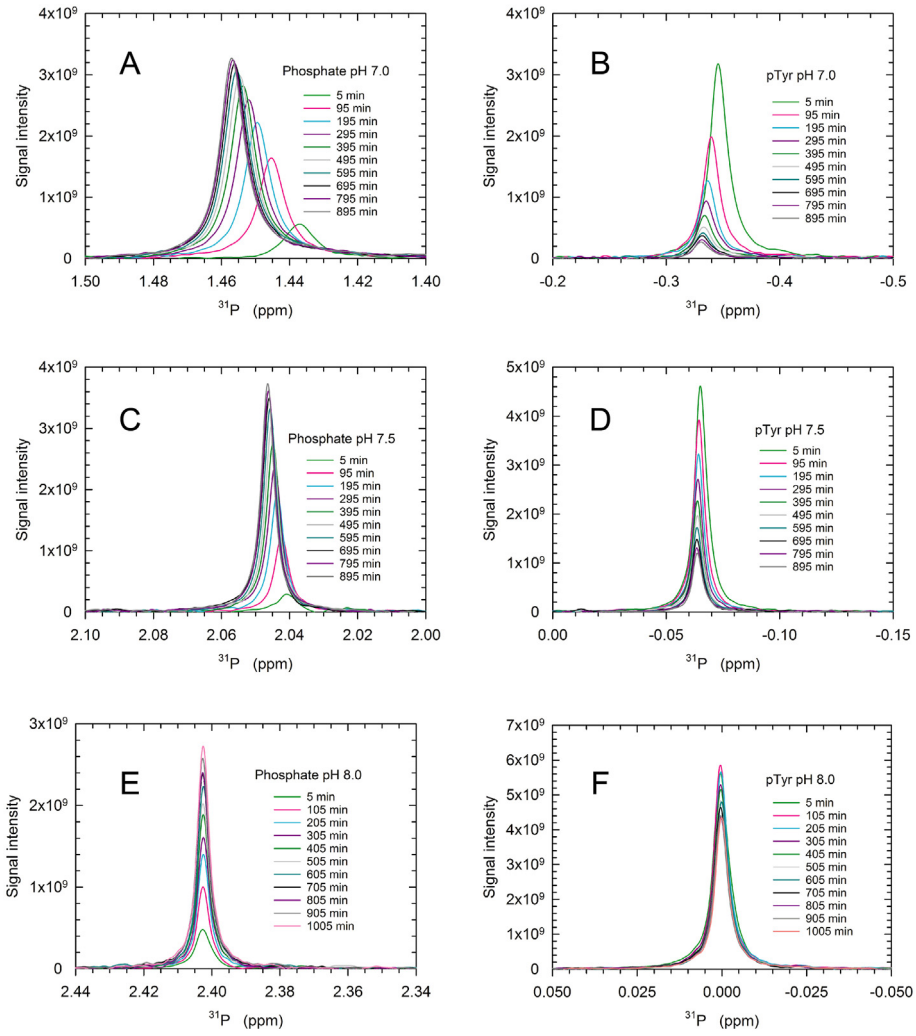

Fig. 6. MptpA-catalyzed hydrolysis of pTyr analysed by NMR spectroscopy
(**A-F**) ^{31}P NMR spectra recorded at 298 K as a function of time using a reaction mixture containing MptpA$_{sW48}$ and pTyr (2 μM and 1.5 mM, respectively) in Tris-HCl/Bis-Tris (50 mM each), 150 mM NaCl, and 1 mM EDTA. Two spectral regions, diagnostic of phosphate generation (panels A, C, and E) and of pTyr consumption (panels B, D, and F) are shown. The pH of the samples was equal to 7.0 (panels A and B), 7.5 (panels C and D) and 8.0 (panels E and F). For the assays at pH 7.0 and 7.5 the spectra were obtained 5, 95, 195, 295, 395, 495, 595, 695, 795, and 895 min after reaction was started (green, magenta, cyan, dark magenta, dark green, grey, dark cyan, black, purple, and dark grey lines, respectively). For the two assays at pH 8.0 the spectra were obtained 5, 105, 205, 305, 405, 505, 605, 705, 805, 905, and 1005 min after reaction was started (green, magenta, cyan, dark magenta, dark green, grey, dark cyan, black, purple, dark grey, and salmon lines, respectively).

Conversely, a significant decrease of ellipticity was detected when MptpA$_{sW48}$ was exposed to pH 6.5, and an even more pronounced decrease was observed at pH 6.0 (Fig. 9A). This observation matches qualitatively the structural changes detected for MptpA$_{sW48}$ by means of high-resolution NMR spectroscopy, mainly characterizing the tertiary fold of this enzyme. Quantitatively speaking, the CD spectrum determined here for MptpA$_{sW48}$ at pH 7.5 features an about 25% lower amplitude when compared to that previously reported for MptpA by Margenat et al. [41]. Moreover, the decrease of mean residue weighted ellipticity detected here by exposing the enzyme to pH 6.0 (Fig. 9A) is similar to the effect induced by the introduction in MptpA of the site-specific mutations C11A, C16A, and C53A whose presence is responsible for a 30% lower α-helical content of the enzyme secondary structure [42]. To evaluate the molar ellipticity of MptpA$_{sW48}$ under strongly denaturing conditions, we determined the CD spectra of solutions containing 1 μM enzyme at pH 6.0 or 7.0, in the presence or in the absence of 8 M urea. Interestingly, the CD spectra of enzyme solutions containing the chaotrope were not affected by pH, indicating that the action of urea on the secondary structure of MptpA$_{sW48}$ does largely dominate the effects triggered by acidic conditions (Fig. 9B). It is also interesting to note that the presence of urea induces a decrease of molar ellipticity at 222 nm equal to approximately 50 and 70% when compared to the observations respectively obtained at pH 7.0 and 6.0 in the absence of the chaotrope (Fig. 9B). Finally, we determined the molar ellipticity of MptpA$_{sW48}$ over a pH interval ranging from 5.0 to 8.0, using samples featuring pH values differing by 0.25 units. Remarkably, the content of secondary structure of the enzyme was found to undergo a quite sharp decrease when the pH was shifted from 6.25 to 6.0 (Fig. 9C). Nevertheless, this decrease is of limited extent when compared to the effect triggered by exposing MptpA$_{sW48}$ to 8 M urea (cf. Fig. 9B and 9C).

These observations imply that the secondary structure of MptpA$_{sW48}$ is only mildly affected by changing the pH between 8.0 and 6.25. Even at pH 5.0 the enzyme is not entirely shifted to an ensemble of unfolded conformations. Indeed, lowering the pH to 6.5 or to lower values induces a significant loss of MptpA$_{sW48}$ tertiary structure of MptpA$_{sW48}$ (according to the data obtained by

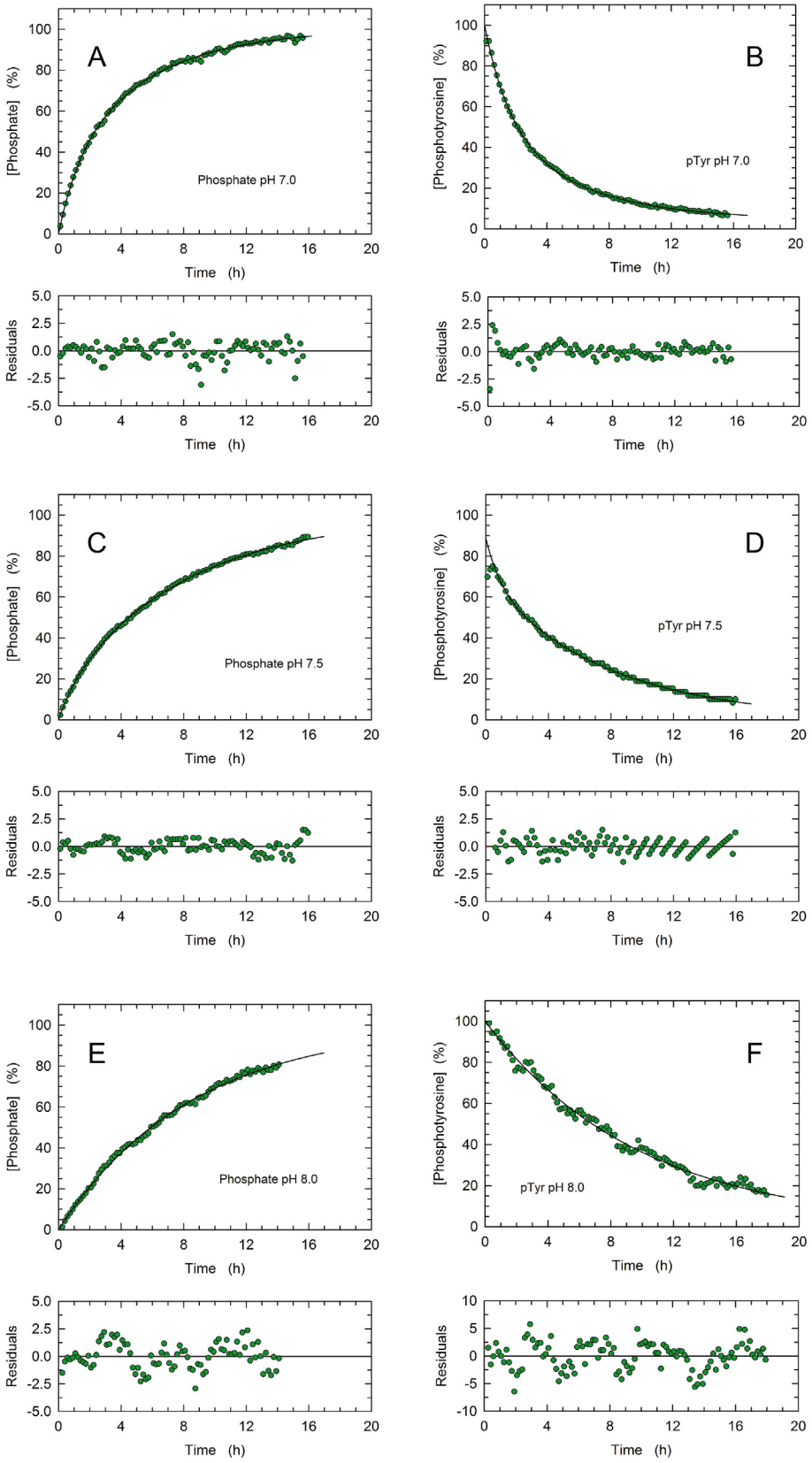

Fig. 7. Kinetics of phosphate generation and pTyr consumption determined by NMR spectroscopy
(**A-F**) Time-course of phosphate and pTyr concentration changes analysed by one-dimensional ^{31}P NMR spectroscopy using reaction mixtures containing MptpA$_{sW48}$ and pTyr (2 μM and 1.5 mM, respectively) in Tris-HCl/Bis-Tris (50 mM each), 150 mM NaCl, and 1 mM EDTA. All assays were performed at 298 K. The kinetics of phosphate generation is reported in panels A, C, and E, and that of pTyr consumption is shown in panels B, D, and F. The pH of the samples was equal to 7.0 (panels A and B), 7.5 (panels C and D) and 8.0 (panels E and F). The continuous lines represent fittings of a double- or single-exponential equation to the experimental observations. Experimental data have been normalized using the maximum of initial (in the case of pTyr) or final (in the case of phosphate) value provided by the function used for data analysis. See Table 4 for the corresponding numerical data.

Table 4
Kinetic rate constants (in units of hours) and normalized amplitudes determined by fitting the indicated equations to the experimental observations obtained by ^{31}P NMR spectroscopy to monitor the decay of substrate and the generation of phosphate during the hydrolysis of pTyr catalyzed by MptpA$_{sW48}$.
Experimental data have been normalized using the maximum of initial (in the case of pTyr) or final (in the case of phosphate) value provided by the function used for data analysis. The corresponding data are shown in Figs. 6 and 7.

pH 7.0	pH 7.5	pH 8.0
Phosphate, f = a•(1-exp^{-bx}) + c•(1-epx-^{dx})	**Phosphate, f = a•(1-exp^{-bx}) + c•(1-epx-^{dx})**	**Phosphate, f = a•(1-exp^{-bx})**
a = 0.30 ± 0.04	a = 0.124 ± 0.015	a = 1.00 ± 0.01
b = 0.79 ± 0.10	b = 0.87 ± 0.15	b = 0.118 ± 0.003
c = 0.70 ± 0.04	c = 0.88 ± 0.01	–
d = 0.187 ± 0.012	d = 0.126 ± 0.005	–
pTyr, f = a•exp^{-bx} + c•exp^{-dx}	**pTyr, f = a•exp^{-bx} + c•exp^{-dx}**	**pTyr, f = a•exp^{-bx}**
a = 0.44 ± 0.06	a = 0.212 ± 0.019	a = 1.00 ± 0.02
b = 0.66 ± 0.06	b = 1.10 ± 0.19	b = 0.102 ± 0.005
c = 0.51 ± 0.05	c = 0.677 ± 0.008	–
d = 0.187 ± 0.020	d = 0.128 ± 0.006	–

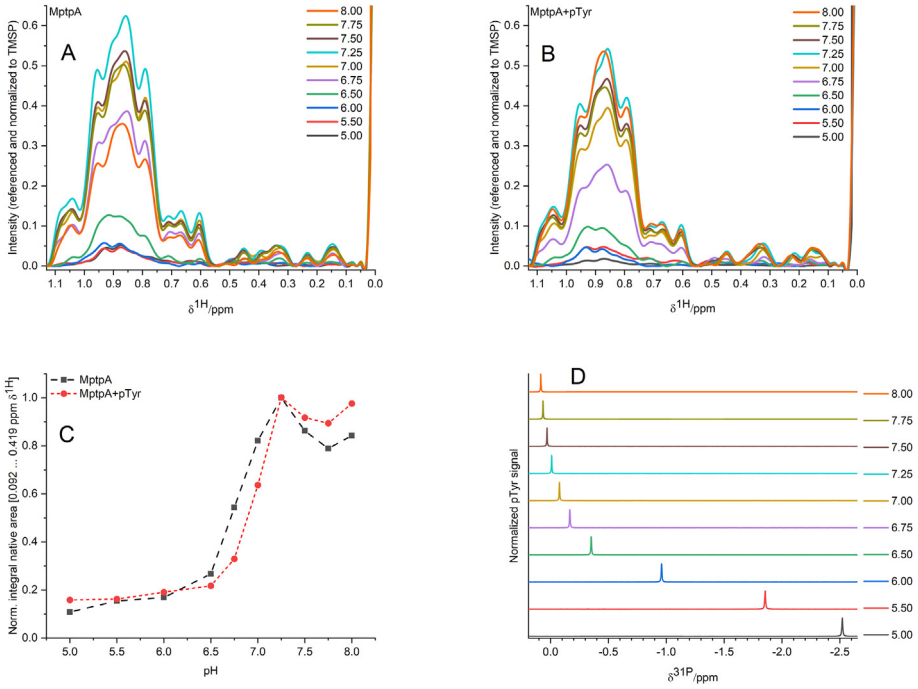

Fig. 8. One-dimensional ^{1}H NMR spectra of MptpA$_{sW48}$ observed at different pH values
(**A-B**) NMR spectra of 60 μM MptpA$_{sW48}$ in Tris-HCl/Bis-Tris (50 mM each), 150 mM NaCl and 1 mM EDTA, acquired at 298 K in the absence (A) or in the presence (B) of 10 mM pTyr. The different samples were probed, as indicated, at pH 5.0, 5.5, 6.0, 6.5, 6.75, 7.0, 7.25, 7.5, 7.75, and 8.0 (black, red, blue, green, magenta, light brown, cyan, brown, ochre, and orange lines, respectively). (**C**) Spectra shown in panels A and B have been integrated over a range of chemical shifts between 0.092 and 0.419 ppm. The data obtained in the absence or in the presence of pTyr are reported with black squares and red circles, respectively. (**D**) Dependence on pH of the resonance signal originating from pTyr in one-dimensional ^{31}P NMR spectra. Specific pH values and color coding as in panels A and B.

NMR spectroscopy), whereas the enzyme secondary structure is essentially preserved (as determined by CD spectroscopy). Thus, we propose that under these conditions MptpA$_{sW48}$ features a molten globule state which is catalytically competent, as shown here (Fig. 1).

3.8. Ionization state of Histidines and MptpA$_{sW48}$ surface electrostatic potential

As previously mentioned, the pH interval considered for the majority of the experiments reported here is rather large, and therefore certainly affects the overall charge of MptpA$_{sW48}$. In particular, it seems reasonably to suppose that shifting the pH from 5.0 to 8.0 the enzyme's histidines undergo a transition from charged to uncharged state, with aspartates/glutamates and lysines/arginines maintaining their charge independently of the pH shift. Accordingly, to test the effect triggered by acidic conditions on the surface-exposed amino acids of MptpA$_{sW48}$, we analysed the electrostatic surface potential (see Methods) of the enzyme under two conditions. To this aim, we used the tertiary structure of MptpA reported by Madhurantakam et al. [30] and we determined (by means of the APBS plugin of PyMol) the electrostatic surface potential of two states of the protein, respectively: i) featuring a total charge unmodified respect to the source PDB file, which is equal to −4; ii) bearing a total charge equal to +6, with this positive net charge obtained by adding a +1 charge to the 10 histidines of MptpA. In our view, this comparison may help to evaluate what the enzyme faces when exposed to pH < 6.5, i.e. to pH values lower than the pKa values of protein histidines. Interestingly enough, we found that the shift from −4 to +6 of the net charge of MptpA induces major changes of the surface electrostatic potential (ESP) on one side only of the enzyme (Fig. 10). In particular, viewing MptpA

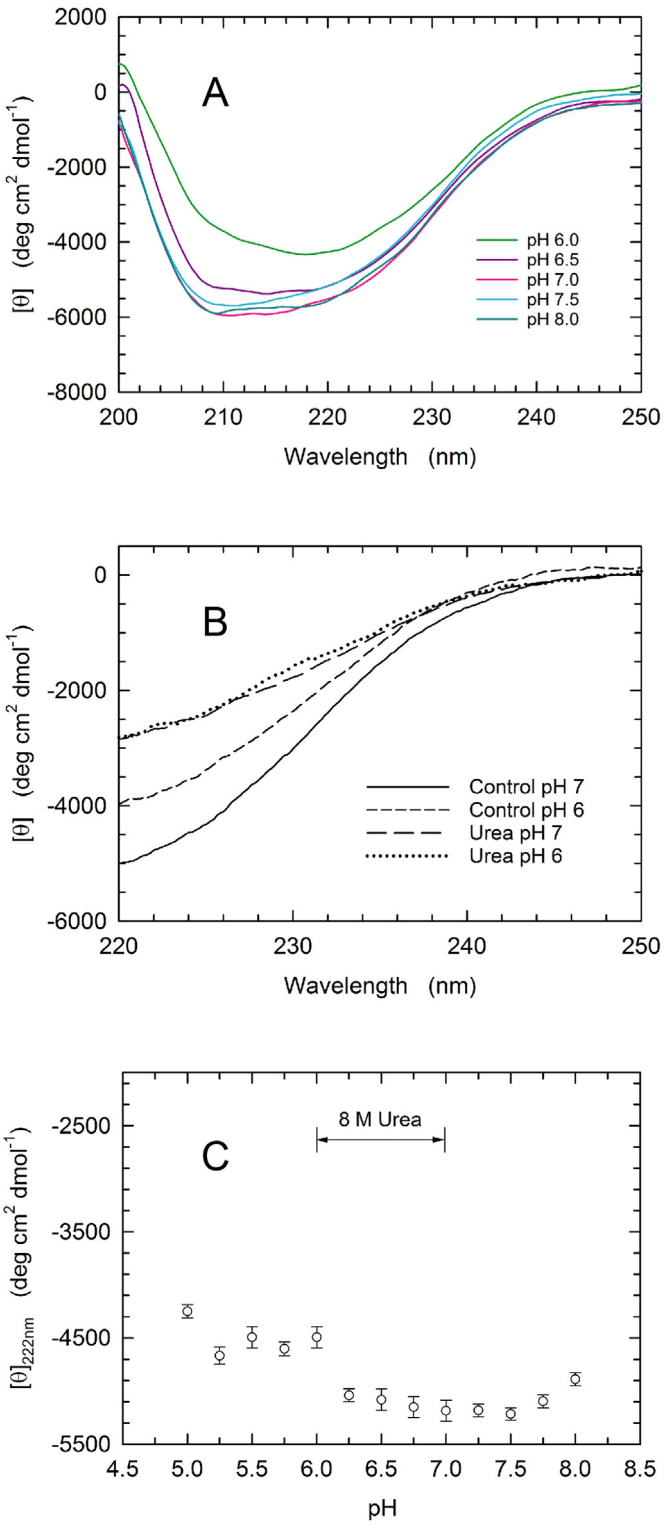

Fig. 9. CD spectra of MptpA$_{sW48}$ in PBS buffer poised at different pH values
(**A**) CD spectra of MptpA$_{sW48}$ in PBS buffer at pH 6.0, 6.5, 7.0, 7.5, and 8.0 (green, purple, magenta, cyan, and dark green lines, respectively). (**B**) CD spectra of MptpA$_{sW48}$ in MES-Tris buffer at pH 6.0 and 7.0, in the absence or in the presence of 8 M urea. (**C**) Mean residue ellipticity of MptpA$_{sW48}$ (in MES-Tris buffer) determined at 222 nm as a function of pH. The mean residue ellipticity of MptpA$_{sW48}$ determined at 222 nm in the presence of 8 M urea is also shown ($[\theta]_{222nm} = -2631$ deg cm^2 dmol^{-1}).

with R159 oriented to the observer (Fig. 10A and 10D) or viewing the enzyme from the top of the active site (Fig. 10C and 10 F), the ESP does slightly diverge when the two enzyme states are compared. On the contrary, viewing MptpA from the side opposite to R159 (Fig. 10 B and 10 E) a conspicuous shift of the ESP is observed. Overall, the calculated changes of ESP appear significant, albeit affecting a limited region of the enzyme. Nevertheless, the shift to a rather positive ESP on one side of the enzyme (Fig. 10B and 10E) may trigger important structural rearrangements, such as those detected by 1D ^{1}H NMR spectra (Fig. 8A and 8B).

4. Discussion

The catalytic action of protein tyrosine phosphatases is usually investigated by activity assays performed using *p*-nitrophenyl phosphate (pNPP) as substrate. Conversely, we report here on the performance of *Mycobacterium tuberculosis* low-molecular weight protein tyrosine phosphatase (MptpA) at the expense of phosphotyrosine (pTyr). In particular, we analysed the pH-dependence of the MptpA$_{sW48}$-catalyzed pTyr hydrolysis, inspecting this reaction from both the substrate and the enzyme side.

Under steady-state conditions, the maximal catalytic effectiveness of MptpA$_{sW48}$ was observed at neutral pH, with the enzyme action being more sensitive to acidic than to alkaline pH (Fig. 1A). This does not fully agree with previous observations obtained with MptpA and pNPP, generating a symmetric bell-shaped curve for the dependence on pH of enzyme activity [43]. Moreover, in the presence of pNPP MptpA obeys Michaelis-Menten kinetics and features an invariance of the K_m value over the 5.0–7.0 pH interval [43], whereas using pTyr we observed here that a decrease of pH from 6.5 to 6.0 triggers a sharp transition from sigmoidal to Michaelis-Menten kinetics and a large increase of enzyme $K_{0.5}$ (Table 1). This apparent discrepancy between previous and our observations can be related to different properties of the phosphate group of pNPP and pTyr. It is important to note that the pKa_1 value of pNPP was reported as equal to 0.21 or 0.30 [44], whereas a value of 0.9 was determined for the pKa_1 of pTyr [45]. Further, and more importantly, the pKa_2 of pNPP was estimated as equal to 4.96 [44], 5.18 [44] or 5.12 ± 0.18 [46], with all these values significantly lower when compared to those relative to the pKa_2 value of pTyr, i.e. 5.55 ± 0.04 [47], 5.8 ± 0.1 [36], 5.67 ± 0.01 (Fig. 2), and 5.76 ± 0.01 (Fig. 2). Therefore, we propose that these properties represent a major determinant of the pH-dependence of MptpA$_{sW48}$ catalytic action at the expense of pNPP [43] and pTyr (Fig. 1A, Table 1), suggesting that the presence of two negative charges in the phosphate group favours substrate binding to the active site of the enzyme. This was confirmed by the Surface Plasmon Resonance experiments reported here (Fig. 3, Table 2), indicating the absence of a detectable binding at pH < 6.0. Moreover, the quite prolonged lag phase (lasting for about 10 s) that was observed before the generation of any reaction product was detectable at pH 6.0 under pre-steady state conditions (Fig. 4A) is also diagnostic of inefficient binding of pTyr by MptpA. To interpret the alkaline limb of the bell-shaped curve relating MptpA$_{sW48}$ activity and pH (Fig. 1A), the data we obtained at pH 8.0 by NMR spectroscopy are of interest. In particular, the fast phase observed when the reaction catalyzed by MptpA$_{sW48}$ was assayed at pH 7.0 or 7.5 was not detected when activity assays were performed at pH 8.0 (Table 4). This suggests that a particular residue of MptpA$_{sW48}$ is engaged in general acid catalysis, as it was shown for aspartate 356 of *Yersinia enterocolitica* PTPase [26]. Accordingly, we propose to ascribe the identity of this general acid catalyst to aspartate 126 of MptpA$_{sW48}$, an amino acid previously shown to be essential for catalysis [43].

The repertoire of inhibitors designed and synthesized against MptpA contains quite a number of representatives exerting a competitive action [48–50]. Conventionally, these inhibitors are tested at pH 7.0 using pNPP as substrate, i.e. under conditions corresponding to maximal enzyme activity. However, it is known

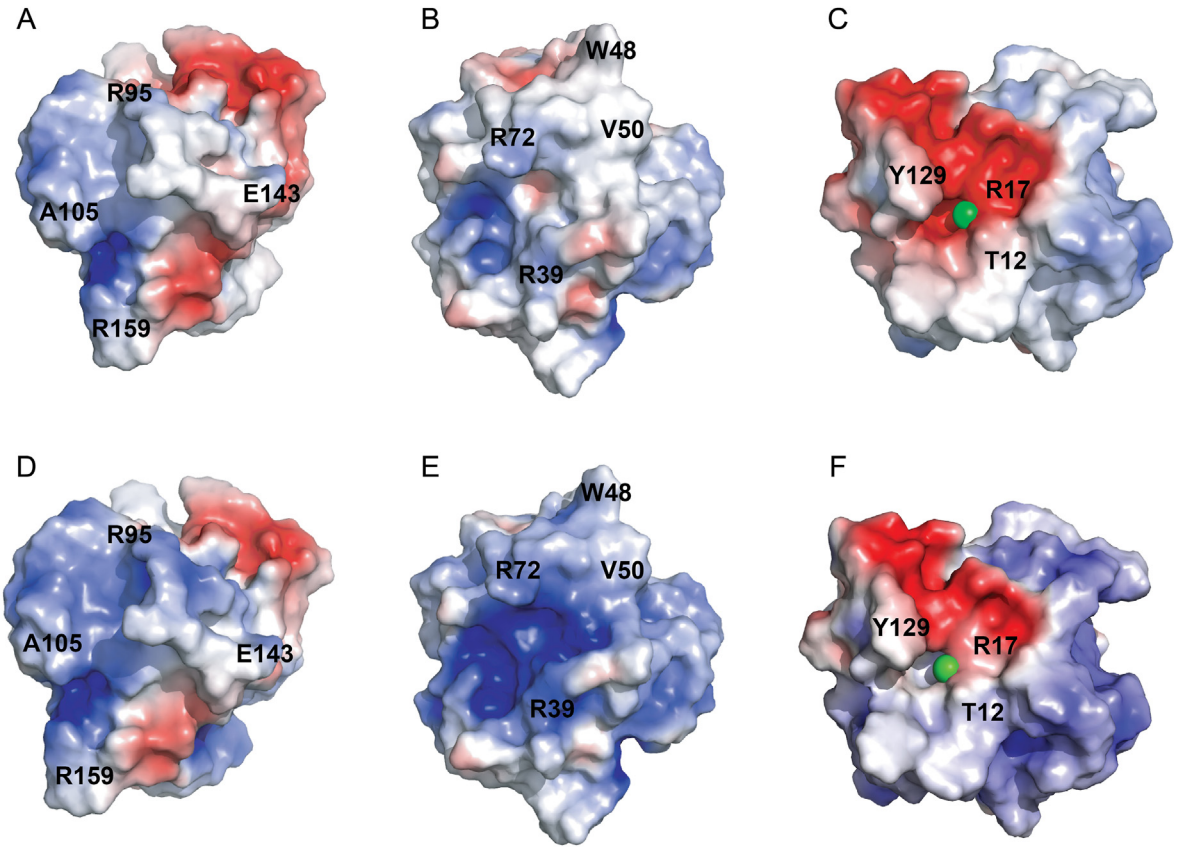

Fig. 10. Surface electrostatic potential of two alternative states of MptpA
(**A-C**) The surface electrostatic potential of MptpA (PDB file 1u2p) was determined using the APBS plugin of PyMol. Each of the three different orientations of the enzyme (A–C) is defined by the indicated amino acids, which are directed to the observer. In particular, the orientations reported in (A) and (B) are reciprocally rotated by 180°. The green sphere in C represent a chloride atom residing in the enzyme active site. (**D-F**) Surface electrostatic potential of MptpA the formal charge of which was modified by assigning to each of the ten histidines a formal charge equal to +1. Enzyme orientations (D–F) as those reported in (A–C).

that macrophages feature an acidic pH, to which *Mycobacterium tuberculosis* is therefore exposed *in vivo* [6]. Accordingly, and considering the relatively high K_m value for pTyr featured by $MptpA_{sW48}$ at pH 6.0 (Table 1), we reasoned that it would be of interest to assay the potent MptpA competitive inhibitor L335-M34 as a function of pH. Interestingly, the highest effectiveness of L335-M34 was observed at pH 6 when compared to the inhibition triggered at pH 7.0 or 8.0 (Fig. 5), suggesting that at acidic pH the inhibitor takes advantage of the poor affinity of MptpA towards pTyr (Tables 1 and 2).

The effect of pH on the hydrolysis of pTyr catalyzed by $MptpA_{sW48}$ was also inspected by one-dimensional ^{31}P NMR spectroscopy. In particular, this approach was invaluable to monitor the reaction kinetics by detecting both the generation of inorganic phosphate and the consumption of pTyr (Fig. 6). Unfortunately, at pH 6.0 the reaction was too slow, hampering its detection by NMR spectroscopic approaches. However, we were able to observe the time-course of pTyr hydrolysis over the pH interval from 7.0 to 8.0, and when the generation of phosphate was investigated, we detected a pronounced displacement of the chemical shift of this reaction product as a function of pH (Fig. 6). Remarkably, the observed extent of this displacement, which is related to the dissociation of $H_2PO_4^-$ into HPO_4^{2-} according to a pKa_2 value equal to 6.82 [51], does quantitatively agree with previous estimations [52,53]. In addition to the pH-induced displacement of the phosphate chemical shift, we also observed a concentration-dependent effect (Fig. 6). This effect can be interpreted by the inverse proportionality occurring between the concentration and the pKa_2 value of phosphate [54], inducing additional dissociation of $H_2PO_4^-$ at neutral and slightly alkaline pH (Fig. 6A, 6C, and 6E). When the consumption of pTyr was analysed by NMR spectroscopy, we detected both pH- and concentration-induced displacement of the chemical shift of this substrate (Fig. 6B, 6D, and 6F), suggesting for these observations the same interpretation as proposed for the release of phosphate from pTyr.

Analysing the kinetics of phosphate generation and pTyr consumption observed by NMR spectroscopic assays, we determined at pH 8.0 kinetic rate constants (for both product generation and substrate consumption) significantly lower when compared to those evaluated at pH 7.0 and 7.5 (Table 4). This is in full agreement with the outcome of the experiments independently performed by UV spectroscopy (Table 1), indicating neutral pH as the optimum for the catalytic action of MptpA. Further, at pH 7.0 and 7.5 the reaction featured biphasic kinetics, whereas at pH 8.0 only a single slow phase was observed (Table 4). One-dimensional proton NMR spectroscopy has also shown that $MptpA_{sW48}$ preserves structural characteristics of the native tertiary fold in a range of pH between 7.0 and 8.0, whereas under acidic conditions the enzyme undergoes prominent structural changes leading to a rather disordered ensemble of conformations. In particular, the tertiary fold of $MptpA_{sW48}$ is significantly impacted at pH $\leq$ 6.5 (Fig. 8C). Moreover, we also investigated by CD spectroscopy the secondary structure of $MptpA_{sW48}$, and we have shown that the mean molar ellipticity of the enzyme decreases when $MptpA_{sW48}$ is exposed to acidic conditions (Fig. 9). However, we note that: i) the decrease of molar ellipticity observed at pH 6.0 corresponds to a reduced α-helical

content, which can be estimated as equal to ca. 75% of that featured by $MptpA_{sW48}$ under neutral or slightly alkaline conditions; ii) the effect induced by 8 M urea on the enzyme secondary structure is significantly more pronounced when compared with the structural changes triggered by exposure of $MptpA_{sW48}$ to pH 6.0 (Fig. 9B); iii) the partial unfolding to which the enzyme undergoes at pH 6.0 does not translate into a significant loss of catalytic action: when assayed at this pH in the presence of 15 mM pTyr, $MptpA_{sW48}$ features a level of activity quite similar to those we detected at $6.5 \leq pH < 8.0$.

5. Conclusions

Overall, the observations reported here on the *Mycobacterium tuberculosis* protein tyrosine phosphatase $MptpA_{sW48}$ indicate that the catalytic performance of this enzyme is severely counteracted by acidic pH conditions. In particular, when exposed to these conditions the enzyme is subjected to conformational rearrangements increasing structural disorder, leading to a poor propensity to bind the substrate phosphotyrosine. To avoid this, the action of MptpA is known to antagonize the phagosomes-lysosomes fusion, the occurrence of which would inhibit the enzyme by its exposure to strongly acidic pH. Remarkably, the outcome of this reciprocal inhibition represents an important determinant of *M. tuberculosis* pathogenicity. We have also shown here that the effectiveness of the MptpA competitive inhibitor L335-M34 is favoured at $pH < 7.0$, taking advantage of poor substrate binding by the enzyme. Accordingly, we hope that our observations on *M. tuberculosis* MptpA will prompt the synthesis of new inhibitors, whose design will be conceived by taking the features of the enzyme reported here into account.

Funding

Financial support by CSGI is greatly acknowledged.

Data availability

The datasets generated during the current study are available from the corresponding author on reasonable request.

Authors contributions

M.K., A.S., C.P., F.I., F.D.P., L.B., V.C., M.L.B., and A.H. performed the experiments. A.H. designed the study and wrote the manuscript.

Declaration of competing interest

The authors declare that there are no competing interests associated with the manuscript.

Acknowledgements

We thank the University of Konstanz for the permanent investment into the NMR infrastructure.

Appendix A. Supplementary data

Supplementary data to this article can be found online at https://doi.org/10.1016/j.biochi.2023.04.014.

References

[1] F. Portaels, S.R. Pattyn, Growth of mycobacteria in relation to the pH of the medium, Ann. Microbiol. (Paris) 133 (1982) 213–221.
[2] D.L. Piddington, A. Kashkouli, N.A. Buchmeier, Growth of *Mycobacterium tuberculosis* in a defined medium is very restricted by acid pH and Mg^{2+} levels, Infect. Immun. 68 (2000) 4518–4522.
[3] R.B. Abramovitch, K.H. Rohde, F. Hsu, D.G. Russell, *aprABC*: a *Mycobacterium tuberculosis* complex-specific locus that modulates pH-driven adaptation to the macrophage phagosome, Mol. Microbiol. 80 (2011) 678–694.
[4] J.J. Baker, B.K. Johnson, R.B. Abramovitch, Slow growth of *Mycobacterium tuberculosis* at acidic pH is regulated by *phoPR* and host-associated carbon sources, Mol. Microbiol. 94 (2014) 56–69.
[5] O.H. Vandal, L.M. Pierini, D. Schnappinger, C.F. Nathan, S. Ehrt, A membrane protein preserves intrabacterial pH in intraphagosomal *Mycobacterium tuberculosis*, Nat. Med. 14 (2008) 849–854.
[6] K. Pethe, D.L. Swenson, S. Alonso, J. Anderson, C. Wang, D.G. Russell, Isolation of *Mycobacterium tuberculosis* mutants defective in the arrest of phagosome maturation, Proc. Natl. Acad. Sci. USA 101 (2004) 13642–13647.
[7] R. Levin, S. Grinstein, J. Canton, The life cycle of phagosome formation, maturation, and resolution, Immunol. Rev. 273 (2016) 156–179.
[8] J.A. Armstrong, P. D'Arcy Hart, Response of cultured macrophages to *Mycobacterium tuberculosis*, with observations on fusion of lysosomes with phagosomes, J. Exp. Med. 134 (1971) 713–740.
[9] D.L. Clemens, M.A. Horwitz, Characterization of the *Mycobacterium tuberculosis* phagosome and evidence that phagosomal maturation is inhibited, J. Exp. Med. 181 (1995) 257–270.
[10] A.J. Crowle, R. Dahl, E. Ross, M.H. May, Evidence that vesicles containing living, virulent *Mycobacterium tuberculosis* or *Mycobacterium avium* in cultured human macrophages are not acidic, Infect. Immun. 59 (1991) 1823–1831.
[11] S. Sturgill-Koszycki, P.H. Schlesinger, P. Chakraborty, P.L. Haddix, H.L. Collins, A.K. Fok, R.D. Allen, S.L. Gluck, J. Heuser, D.G. Russell, Lack of acidification in *Mycobacterium* phagosomes produced by exclusion of the vesicular proton-ATPase, Science 263 (1994) 678–681.
[12] S. Xu, A. Cooper, S. Sturgill-Koszycki, T. van Heyningen, D. Chatterjee, I.M. Orme, P. Allen, D.G. Russell, Intracellular trafficking in *Mycobacterium tuberculosis* and *Mycobacterium avium*-infected macrophages, J. Immunol. 153 (1994) 2568–2578.
[13] S.C. Cowley, R. Babakaiff, Y. Av-Gay, Expression and localization of the *Mycobacterium tuberculosis* protein tyrosine phosphatase PtpA, Res. Microbiol. 153 (2002) 233–241.
[14] N.K. Tonks, Protein tyrosine phosphatases: from genes, to function, to disease, Nat. Rev. Mol. Cell Biol. 7 (2006) 833–846.
[15] S. Verma, S. Sharma, Protein tyrosine phosphatase as potential therapeutic target in various disorders, Curr. Mol. Pharmacol. 11 (2018) 191–202.
[16] I. Bölin, H. Wolf-Watz, The plasmid-encoded Yop2b protein of *Yersinia pseudotuberculosis* is a virulence determinant regulated by calcium and temperature at the level of transcription, Mol. Microbiol. 2 (1988) 237–245.
[17] J.B. Bliska, K.L. Guan, J.E. Dixon, S. Falkow, Tyrosine phosphatase hydrolysis of host proteins by an essential *Yersinia* virulence determinant, Proc. Natl. Acad. Sci. USA 88 (1991) 1187–1191.
[18] H. Bach, K.G. Papavinasasundaram, D. Wong, Z. Hmama, Y. Av-Gay, *Mycobacterium tuberculosis* virulence is mediated by PtpA dephosphorylation of human vacuolar protein sorting 33B, Cell Host Microbe 3 (2008) 316–322.
[19] J. Castandet, J.F. Prost, P. Peyron, C. Astaire-Dequeker, E. Anes, A.J. Cozzone, G. Griffiths, I. Maridonneau-Parini, Tyrosine phosphatase MptpA of *Mycobacterium tuberculosis* inhibits phagocytosis and increases actin polymerization in macrophages, Res. Microbiol. 156 (2005) 1005–1013.
[20] D. Wong, H. Bach, J. Sun, Z. Hmama, Y. Av-Gay, *Mycobacterium tuberculosis* protein-tyrosine phosphatase (PtpA) excludes host vacuolar H^+-ATPase to inhibit phagosome acidification, Proc. Natl. Acad. Sci. USA 108 (2011) 19371–19376.
[21] Z.Y. Zhang, J.E. Dixon, Active site labelling of the *Yersinia* protein tyrosine phosphatase: the determination of the pK_a of the active site cysteine and the function of the conserved histidine 402, Biochemistry 32 (1993) 9340–9345.
[22] K. Guan, J.E. Dixon, Evidence for protein-tyrosine phosphatase catalysis proceeding via a cysteine-phosphate intermediate, J. Biol. Chem. 266 (1991) 17026–17030.
[23] K. Guan, J.E. Dixon, Protein tyrosine phosphatase activity of an essential virulence determinant in *Yersinia*, Science 249 (1990) 553–556.
[24] Z. Zhang, Y. Wang, L. Wu, E.B. Fauman, J.A. Stuckey, H.L. Schubert, M.A. Saper, J.E. Dixon, The $Cys(X)_5Arg$ catalytic motif in phosphodiester hydrolysis, Biochemistry 33 (1994) 15266–15270.
[25] J.A. Stuckey, H.L. Schubert, E.B. Fauman, Z. Zhang, J.E. Dixon, M.A. Saper, Crystal structure of Yersinia protein tyrosine phosphatase at 2.5 Å and the complex with tungstate, Nature 370 (1994) 571–575.
[26] Z. Zhang, Y. Wang, J.E. Dixon, Dissecting the catalytic mechanism of protein-tyrosine phosphatases, Proc. Natl. Acad. Sci. USA 91 (1994) 1624–1627.
[27] D. Barford, A.J. Flint, N.K. Tonks, Crystal structure of human protein tyrosine phosphatase 1B, Science 263 (1994) 1397–1404.
[28] Z. Jia, D. Barford, A.J. Flint, N.K. Tonks, Structural basis for phosphotyrosine peptide recognition by protein tyrosine phosphatase 1B, Science 268 (1995) 1754–1758.
[29] T. Stehle, S. Sreeramulu, F. Löhr, C. Richter, K. Saxena, H.R.A. Jonker, H. Schwalbe, The apo-structure of the low molecular weight protein-tyrosine phosphatase A (MptpA) from *Mycobacterium tuberculosis* allows for better target-specific drug development, J. Biol. Chem. 287 (2012) 34569–34582.
[30] C. Madhurantakam, E. Rajakumara, P.A. Mazumdar, B. Saha, D. Mitra, H.G. Wiker, R. Sankaranarayanan, A.K. Das, Crystal structure of low molecular

weight protein-tyrosine phosphatase from *Mycobacterium tuberculosis* at 1.9 Å resolution, J. Bacteriol. 187 (2005) 2175–2182.
[31] A. Stefan, F. Dal Piaz, A. Girella, A. Hochkoeppler, Substrate activation of the low-molecular weight protein tyrosine phosphatase from *Mycobacterium tuberculosis*, Biochemistry 59 (2020) 1137–1148.
[32] N.K. Dutta, R. He, M.L. Pinn, Y. He, F. Burrows, Z. Zhang, P.C. Karakousis, Mycobacterial protein tyrosine phosphatases A and B inhibitors augment the bactericidal activity of the standard anti-tuberculosis regimen, ACS Infect. Dis. 2 (2016) 231–239.
[33] M.M. Bradford, A rapid and sensitive method for the quantitation of microgram quantities of protein utilizing the principle of protein-dye binding, Anal. Biochem. 72 (1976) 248–254.
[34] F. Dal Piaz, A. Vassallo, M.G. Chini, F.M. Cordero, F. Cardona, C. Pisano, G. Bifulco, N. De Tommasi, A. Brandi, Natural iminosugar (+)-lentiginosine inhibits ATPase and chaperone activity of Hsp90, PLoS One 7 (2012), e43316.
[35] B.T. Burlingham, T.S. Widlanski, An intuitive look at the relationship of K_i and IC_{50}: a more general use of the Dixon plot, J. Chem. Educ. 80 (2003) 214–218.
[36] J.M. Bradshaw, G. Waksman, Calorimetric investigation of proton linkage by monitoring both the enthalpy and association constant of binding: application to the interaction of the Src SH2 domain with a high-affinity tyrosyl phosphopeptide, Biochemistry 37 (1998) 15400–15407.
[37] I. Apostol, R. Kuciel, E. Wasylewska, W.S. Ostrowski, Phosphotyrosine as a substrate of acid and alkaline phosphatases, Acta Biochim. Pol. 32 (1985) 187–197.
[38] C.A. Peloquin, G.R. Davies, The treatment of tuberculosis, Clin. Pharmacol. Ther. 110 (2021) 1455–1466.
[39] B. Köhn, M. Kovermann, All atom insights into the impact of crowded environments on protein stability by NMR spectroscopy, Nat. Commun. 11 (2020) 5760.
[40] B. Köhn, M. Kovermann, Macromolecular crowding tunes protein stability by manipulating solvent accessibility, Chembiochem 20 (2019) 759–763.
[41] M. Margenat, A. Labandera, M. Gil, F. Carrion, M. Purificação, G. Razzera, M.M. Portela, G. Obal, H. Terenzi, O. Pritsch, R. Durán, A.M. Ferreira, A. Villarino, New potential eukaryotic substrates of the mycobacterial protein tyrosine phosphatase PtpA: hints of a bacterial modulation of macrophage bioenergetics state, Sci. Rep. 5 (2015) 8819.
[42] C. Matiollo, G. Ecco, A.C.O. Menegatti, G. Razzera, J. Vernal, H. Terenzi, S-nitrosylation of *Mycobacterium tuberculosis* tyrosine phosphatase A (PtpA) induces its structural instability, Biochim. Biophys. Acta 1834 (2013) 191–196.
[43] C. Madhurantakam, V.R.M. Chavali, A.K. Das, Analyzing the catalytic mechanism of MptpA: a low molecular weight protein tyrosine phosphatase from *Mycobacterium tuberculosis* through site-directed mutagenesis, Proteins 71 (2008) 706–714.
[44] N. Bourne, A. Williams, Effective charge on oxygen in phosphoryl (-PO_3^{2-}) group transfer from an oxygen donor, J. Org. Chem. 49 (1984) 1200–1204.
[45] M. Edelson-Averbukh, A. Shevchenko, R. Pipkorn, W.D. Lehman, Gas-phase intramolecular phosphate shift in phosphotyrosine-containing peptide monoanions, Anal. Chem. 81 (2009) 4369–4381.
[46] Z. Zhang, W.P. Malachowski, R.L. Van Etten, J. Dixon, Nature of the rate-determining steps of the reaction catalyzed by the Yersinia protein-tyrosine phosphatase, J. Biol. Chem. 269 (1994) 8140–8145.
[47] P.L. Robitaille, P.A. Robitaille, G.G. Brown Jr., G.G. Brown, An analysis of the pH-dependent chemical-shift behaviour of phosphorous-containing metabolites, J. Magn. Reson. 92 (1991) 73–84.
[48] A.P.G. Silva, L. Tabernero, New strategies in fighting TB: targeting *Mycobacterium tuberculosis*-secreted phosphatases MptpA & MptpB, Future Med. Chem. 2 (2010) 1325–1337.
[49] L. Fanzani, F. Porta, F. Meneghetti, S. Villa, A. Gelain, A.P. Lucarelli, E. Parisini, *Mycobacterium tuberculosis* low molecular weight phosphatases (MptpA and MptpB): from biological insight to inhibitors, Curr. Med. Chem. 22 (2015) 3110–3132.
[50] K.V. Ruddraraju, D. Aggarwal, Z. Zhang, Therapeutic targeting of protein tyrosine phosphatases from *Mycobacterium tuberculosis*, Microorganisms 9 (2021) 14.
[51] W.D. Kumler, J.J. Eiler, The acid strength of mono and diesters of phosphoric acid. The *n*-alkyl esters from methyl to butyl, the esters of biological importance, and the natural guanidine phosphoric acids, J. Am. Chem. Soc. 65 (1943) 2355–2361.
[52] F. Dayrit, E.Q. Espiritu, N. Gonzalez, N. Rojas, J.T. Aguilan, A.M. Basilio, E.T. Chainani, E. Cruz, B. Matanguihan, Development of ^{31}P nuclear magnetic resonance methods for the study of phosphate metabolisms in *E. coli* and *B. subtilis*, Kimika 15 (1999) 9–15.
[53] K.C. Wong-Moon, X. Sun, X.C. Nguyen, B.P. Quan, K. Shen, P.A. Burke, NMR spectroscopic evaluation of the internal environment of PLGA microspheres, Mol. Pharm. 5 (2008) 654–664.
[54] A.A. Green, The preparation of acetate and phosphate buffer solutions of known P_H and ionic strength, J. Am. Chem. Soc. 55 (1933) 2331–2336.